Computers and Chemical Engineering 201 (2025) 109200

Contents lists available at ScienceDirect

Computers and Chemical Engineering

journal homepage: www.elsevier.com/locate/cace

Retrofitting Ordinary Portland cement production for reduced greenhouse gas emissions

Ariana Y. Ojeda-Paredes [a,b], Alexander Mitsos [c,a,d], Manuel Dahmen [a,*]

[a] Forschungszentrum Jülich GmbH, Institute of Climate and Energy Systems, Energy Systems Engineering (ICE-1), Jülich 52425, Germany
[b] RWTH Aachen University, Aachen, 52062, Germany
[c] JARA-ENERGY, Jülich 52425, Germany
[d] RWTH Aachen University, Process Systems Engineering (AVT.SVT), Aachen 52074, Germany

ARTICLE INFO

Keywords:
Cement production
Ordinary Portland cement
Superstructure optimization
Carbon utilization
Carbon storage

ABSTRACT

Cement production is an energy-intensive process and a major greenhouse gas (GHG) emitter. Carbon capture, utilization and storage (CCUS) technologies and fossil fuel substitution have been studied as carbon mitigation measures in the cement industry. However, their optimal combination for retrofitting the production of Ordinary Portland cement (OPC) has yet to be assessed. We formulate and optimize a superstructure to retrofit the OPC production by optimally combining CCUS technologies and fuel switching. Our analysis shows that the emerging Pareto-optimal designs heavily depend on the local conditions, notably the availability of biomass and carbon storage, electricity prices, and emission factor of the used electricity mix. Economically, carbon capture and storage (CCS) is more cost-effective than carbon capture and utilization (CCU) via power-to-methane at current costs in Germany. Only if renewable electricity can be accessed at very low cost, CCU becomes an attractive option.

1. Introduction

Cement production is an energy-intensive process and, primarily due to clinker production, accounts for about 7% of global CO_2 emissions (International Energy Agency (IEA), 2018). Specifically, around 1 tonne of CO_2 is released per tonne of grey clinker by the combustion of fossil fuels in the pyroprocessing stage and by the calcination of limestone to produce clinker (Schorcht et al., 2013). Therefore, various carbon mitigation initiatives have been devised (Ishak and Hashim, 2015; International Energy Agency (IEA), 2018; Hasanbeigi et al., 2012), e.g., applying carbon capture technologies, using alternative fuels, producing alternative binders, and improving energy efficiency.

Carbon capture technologies for cement plants are often categorized based on their technology readiness level (TRL). Promising technologies are chemical absorption and calcium looping at TRL 7 to 8 and oxyfuel combustion and direct separation at TRL 5 to 6 (International Energy Agency (IEA), 2020). To date, carbon capture technologies have not been deployed on a commercial scale in the cement industry (Bacatelo et al., 2023). In fact, there is no large-scale implementation in operating clinker production plants, but several pilot projects have applied these technologies on a partial scale with a view to industrial scale (Perilii, 2021). For instance, the European Cement Research Academy (ECRA) has conducted oxyfuel combustion investigations since 2007 and started an industrial oxyfuel carbon capture project at HeidelbergCement's Colleferro plant in Italy and LafargeHolcim's Retznei plant in Austria in 2018 (Plaza et al., 2020). Additionally, the Low Emissions Intensity Lime and Cement (LEILAC) project started up a CO_2 separation pilot plant (LEILAC1) utilizing direct separation as a carbon capture technology, with a capacity of 25 kilotonnes per year. The subsequent phase, LEILAC2, aims to capture approximately four times the capacity of LEILAC1 and is projected to be finalized by 2025 (HeidelbergCement, 2020). Another initiative, the Cleanker project, initiated in 2017, conducts pilot-scale tests at Buzzi Unicem to evaluate the applicability of the entrained flow calcium looping technology (Plaza et al., 2020). HeidelbergCement's Norcem in Norway aims to capture and store all its process CO_2 emissions, around 0.4 Mtonne/year, by applying chemical absorption with an amine solvent (Knudsen, 2019). Carbon capture implementation is indispensable for decarbonizing cement clinker production, as about 60 percent of total CO_2 emissions originate from the calcination of limestone (Toktarova et al., 2020).

Captured CO_2 can be transported through pipelines for geological storage in onshore or offshore saline aquifers (Smith et al., 2021) or used as a feedstock, e.g., for producing chemicals and synthetic fuels by power-to-chemicals/fuels processes (International Energy Agency (IEA), 2018). For instance, power-to-methane (PtMe) utilizes CO_2 and

* Corresponding author.
E-mail address: m.dahmen@fz-juelich.de (M. Dahmen).

https://doi.org/10.1016/j.compchemeng.2025.109200
Received 20 December 2024; Received in revised form 8 May 2025; Accepted 18 May 2025
Available online 5 June 2025

Nomenclature

Abbreviations

AEL	Alkaline electrolysis
ASU	Air separation unit
BAT	Best Available Technique
BIO	Biological methanation
CAPEX	Capital expenditures
CAT	Catalytic methanation
CCS	Carbon capture and storage
CCU	Carbon capture and utilization
CCUS	Carbon capture, utilization and storage
CEPCI	Chemical engineering plant cost index
CPU	Carbon purification unit
GHG	Greenhouse gas
GWI	Global warming impact
LHV	Lower heating value
MEA	Monoethanolamine
MILP	Mixed integer linear programming
OPC	Ordinary Portland cement
OPEX	Operational expenditures
PEMEL	Proton exchange membrane electrolysis
PtG	Power-to-gas
PtH_2	Power-to-hydrogen
PtMe	Power-to-methane
SNG	Synthetic natural gas
SOEL	Solid oxide electrolysis
TAC	Total annualized cost
TRL	Technology readiness level
WACC	Weighted average cost of capital

Greek symbols

α	Scale factor
ΔH	Enthalpy of reaction
ΔT	Temperature difference
η	Efficiency
ν	Stoichiometric ratio
ζ	Splitter fraction

Latin symbols

$\mathcal{A}$	Set of combustors
$\mathcal{B}$	Set of calciners
$\mathcal{C}$	Set of components
c	Heat capacity
CE	CEPCI value
CRF	Capital recovery factor
CS	Credits
CX	Capital costs
D	Size of component
$\mathcal{E}$	Set of electricity-based components
$\mathcal{E}_u$	Set of reactants
$\dot{E}$	Energy flow
EF	Emission factor
EM	CO_2 emissions
$\mathcal{F}$	Set of fuels
f	Fraction of theoretical emissions mitigation potential from SNG production
$\mathcal{G}_u$	Set of products
GWI	Global warming impact
$\mathcal{H}$	Set of thermal components
i	Interest rate of investment
$\mathcal{K}$	Set of species
$\mathcal{L}$	Set of splitters
$\mathcal{M}$	Set of material sources
$\dot{M}$	Material flow
$\mathcal{N}$	Set of sinks
n	Lifetime of the project
$\mathcal{O}$	Set of other componentes
OX	Operating costs
p	Commodity/certificates price
R_{SNG}	Revenues
r_{SNG}	SNG selling price
$\mathcal{S}$	Set of sources and sinks
$\dot{S}$	Energy or material flow from source or to sink
T	Maintenance cost factor
$\mathcal{U}$	Set of conversion units
$\mathcal{X}$	Set of mixers
w	Molecular weight
x	Decision to install component
y	Mass fraction

Subscripts

a	Combustor unit
b	Calciner unit
bCO_2	Biogenic CO_2 emitted
bio	Biomass
c	Component
e	Reactant
el	Electricity
eq	Equivalent
f	Fuel
g	Product
h	Thermal unit
i	Energy/material input stream
j	Energy/material output stream
k	Species
l	Splitter
lime	Limestone
m	Mass source
n	Sink
s	Commodity
$stoCO_2$	Stored CO_2
u	Conversion unit
x	Mixer

Superscripts

capt	Captured
dir	Direct
fix	Fixed
fos	Fossil
in	Input
ind	Indirect
max	Maximum

min	Minimum
nom	Nominal
out	Output
ref	Reference
var	Variable

H_2 from water electrolysis to produce synthetic natural gas (SNG), a gas mixture consisting mainly of methane that can be used for various applications in the residential sector, power generation or industry (Ghaib and Ben-Fares, 2018).

Replacing conventional fossil fuels with low-carbon alternatives reduces the CO_2 intensity of the thermal energy demand in cement production (International Energy Agency (IEA), 2018). Hydrogen from water electrolysis is a potential carbon-neutral fuel for industrial processes to reduce the dependency on fossil fuels (Juangsa et al., 2022) and can provide high-temperature heat, e.g., in copper, iron, and steel production (Röben et al., 2021; Karakaya et al., 2018). Hydrogen has also been studied as an alternative fuel in cement manufacturing, supplementing other fuels like natural gas (Volker Schneider et al., 2016). In 2019, CEMEX initiated trials with hydrogen at its Alicante plant in Spain and later implemented hydrogen technology across all its European plants (CEMEX, 2021). It has been estimated that the adoption of power-to-hydrogen (PtH_2) in the cement industry could potentially lower greenhouse gas (GHG) emissions by approximately 40% (Ishak and Hashim, 2015). Biomass may be considered a carbon-neutral fuel, as the amount of CO_2 released during combustion is assumed to be equivalent to the amount captured from the atmosphere by the biomass during biomass growth (Abbasi and Abbasi, 2010). The most common types of biomass used as fuels in cement production are wood waste and other wastes generated by agricultural and forestry processes (International Energy Agency (IEA) Bioenergy, 2021). Particularly, Hossain et al. (2019) have shown that wood derived fuels are technically and environmentally suitable for use as a co-fuel in cement production. According to International Energy Agency (IEA) (2023), seven cement plants, including the Brevik Norcem plant in Norway, the Cementa Slite plant in Sweden, and the K6 Lumbres project in France, are planning to use biomass feedstocks as bioenergy in the clinker production process and retrofit their plants with carbon capture, utilization, and storage (CCUS) technologies.

CO_2 capture technologies for cement production have been studied and compared from a technical point of view, e.g., with regard to their retrofit potential, emission reduction, and energy efficiency (Voldsund et al., 2019), and economic potential, e.g., avoided cost for CO_2 certificates (Gardarsdottir et al., 2019). The combination of carbon capture and utilization (CCU) technologies, e.g., oxyfuel combustion with power-to-gas (PtG) (Faria et al., 2022), as well as the combination with carbon capture and storage (CCS), e.g., integrated calcium looping with CO_2 storage or chemical absorption with CO_2 storage (Naranjo et al., 2011), have also been investigated. Implementing CCUS technologies for retrofitting cement plants is therefore deemed technically feasible (International Energy Agency-Greenhouse Gas R&D Programme (IEA-GHG), 2013).

Until now, the optimal integration of the various GHG emission reduction technologies has not been assessed. In order to evaluate the economic and environmental potential of retrofitting Ordinary Portland cement (OPC) production with CCUS technologies and find the best combination of technologies, we follow a superstructure optimization approach. A superstructure comprises technological alternatives in the form of unit operations and interconnections. In superstructure optimization, a mathematical program is solved to obtain an optimal process design. This approach is established since decades in chemical engineering, e.g., for utility systems (Papoulias and Grossmann, 1983), isothermal reactor-separator-recycle systems (Kokossis and Floudas, 1991), complex distillation columns (Grossmann et al., 2004) and emerging sustainable processes (Grossmann and Guillén-Gosálbez, 2010). In the field of carbon capture utilization and storage, Lee et al. (2016) identified the cost optimal design of an amine-based carbon capture process using superstructure optimization. Uebbing et al. (2020) applied superstructure optimization to the design of a PtMe process including heat integration. Kenkel et al. (2021) presented a superstructure modeling approach applied to a power-to-methanol process.

Our proposed superstructure optimization model includes commonly discussed mid- and high-TRL technologies for (a) carbon capture, i.e., chemical absorption, calcium looping, oxyfuel combustion, and direct separation, (b) carbon utilization, i.e., alkaline and polymer exchange membrane electrolysis, catalytic and biological methanation, (c) heat supply by coal, biomass, natural gas and PtH_2, and (d) carbon storage. The different technology options are categorized and illustrated in Fig. 1. The model is set up as an optimization problem that minimizes total annualized costs (TAC) of the energy- and emissions-related measures and the global warming impact (GWI) in a bi-objective optimization. Furthermore, we perform a sensitivity analysis to assess the impact of critical economic parameters on the emerging Pareto-optimal designs.

The remainder of this paper is structured as follows: Section 2 provides a concise overview of OPC production, the technologies under consideration for retrofitting OPC production to reduce GHG emissions, and the corresponding main assumptions and parameters for modeling. Section 3 describes the superstructure model and the solution approach. Section 4 introduces different scenarios and analyzes the resulting Pareto-optimal designs. Finally, Section 5 offers concluding remarks.

2. Reference plant and retrofit options

This section provides an overview of the reference OPC production plant considered in this study (Section 2.1) and a brief discussion of the different technology options included in the superstructure (Section 2.2), together with the necessary assumptions and parameters. Section 2.3 surveys the possible fuels to provide the process heat.

2.1. Ordinary Portland Cement (OPC) production

Similar to other studies, see Voldsund et al. (2019) and Quevedo Parra and Romano (2023), we base our reference process on a Best Available Technique (BAT) plant (Schorcht et al., 2013) with a production of 3000 tonnes of clinker per day or approximately 1.14 Mtonnes of cement per year, as illustrated in Fig. 2, assuming an operational period of 330 days per year (Gardarsdottir et al., 2019). Although more than ten years have passed since (Schorcht et al., 2013) published the BAT design, we assume that the design still reflects a reasonable reference design of an OPC production based on conventional fuels. We consider a dry production process, neglecting the moisture from raw materials. The raw material preparation is the first process stage, where a crushing unit transforms the quarried limestone, assumed as 100% $CaCO_3$, into crushed limestone. The crushed limestone is then milled with clay to obtain a raw meal. Following the pyroprocessing stage, the raw meal enters the preheating step, where the flue gases from the rotary kiln are used to preheat the meal. In the subsequent calcination step hard coal is used to provide heat for the limestone calcination reaction. The clinkerization reaction then takes place in the rotary kiln (Schorcht et al., 2013), where the calcium carbonate in the limestone is transformed into calcium oxide and carbon dioxide and clinker is produced with an established composition (Khurana et al., 2002). The hot clinker is discharged into the cooler where it is rapidly quenched. In the last step, the cooled clinker is ground with additional gypsum to produce cement. Voldsund et al. (2019) estimates that only 4% of the steam required in chemical absorption technology can be supplied from heat integration of the flue gas from the cement plant. Therefore, we neglect the option of heat integration in the superstructure. Parameters of the reference production process relevant for the superstructure model are shown in Table 1.

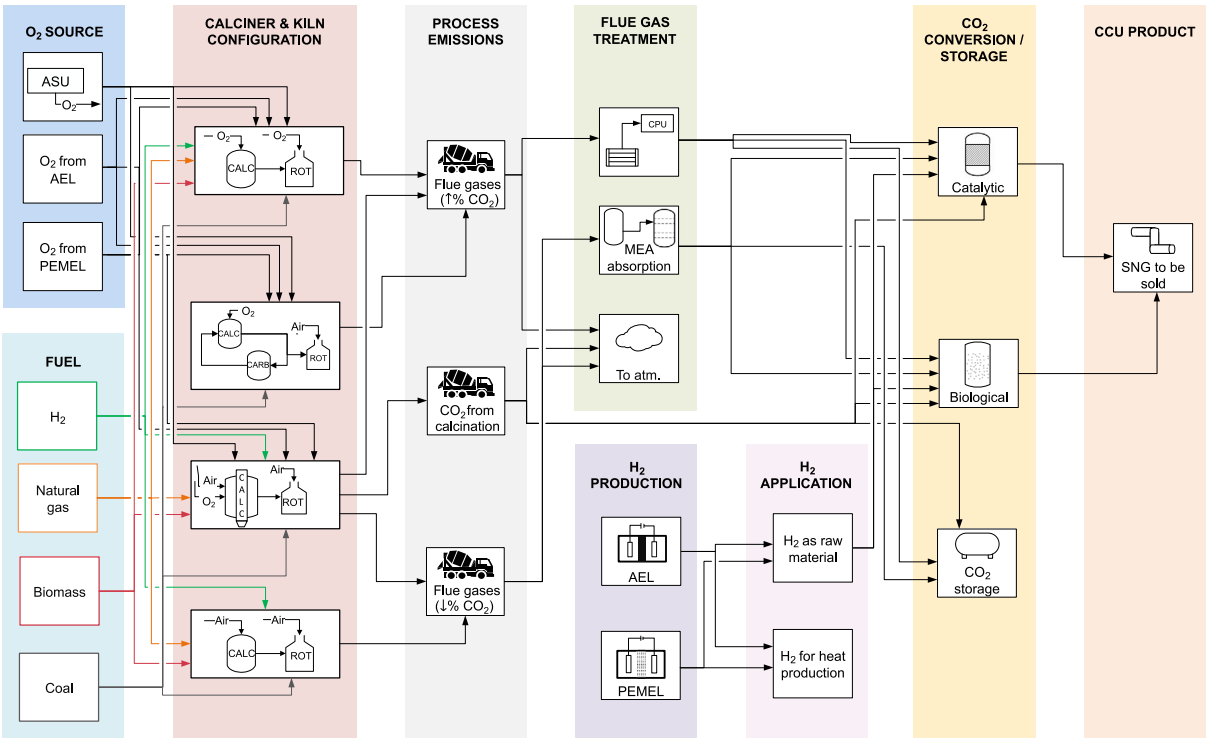

Fig. 1. Technology options for retrofitting OPC production considered in the superstructure optimization approach. Process emissions from oxyfuel combustion have a higher CO_2 content compared to emissions from air combustion, where nitrogen is present and in higher proportion than CO_2.

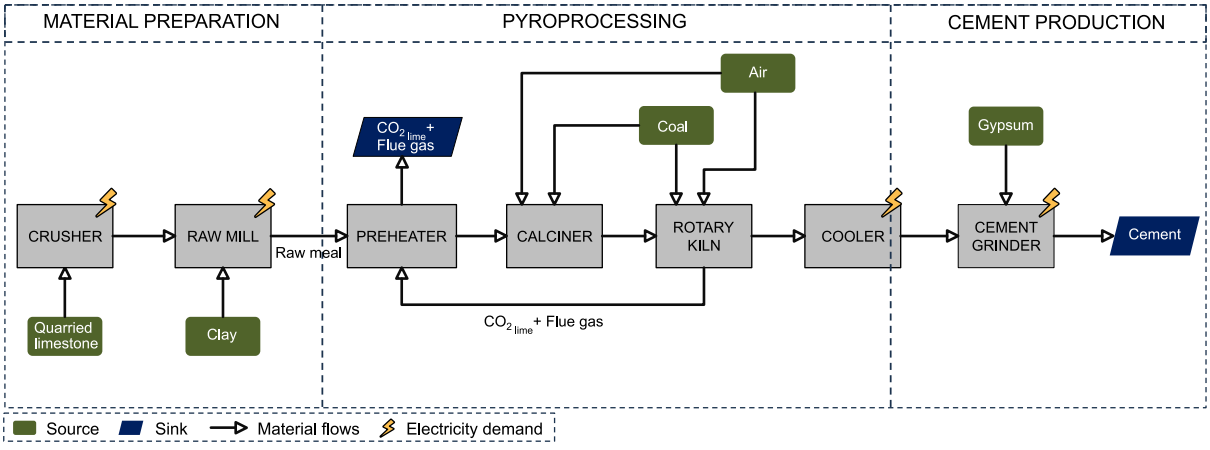

Fig. 2. Flowsheet of a reference OPC production (dry process) operating with coal based on a best available technique (BAT) plant (Schorcht et al., 2013).

Table 1
Reference OPC production parameters.

Component	Value	Unit	Reference
Clinker demand	3000	t/day	Schorcht et al. (2013)
Clinker/cement ratio	0.96	[−]	assuming OPC (CEM I)
Raw meal/clinker ratio	1.56	[−]	assuming limestone is 100% $CaCO_3$
Calcination temperature	900	°C	Deolalkar (2009)
Clinkerization temperature	1450	°C	Deolalkar (2009)

2.2. Retrofit options

Fig. 3 shows the retrofit technologies potentially installed and their integration into the OPC production process via the interconnections between unit operations, sources, and sinks. This subsection briefly describes the technological options and the relevant assumptions and parameters considered, in addition to the description of the sources and sinks.

2.2.1. Chemical absorption

Chemical absorption is an end-of-pipe technology and its integration into a cement plant is relative straightforward since the cement manufacturing process is not directly affected (Hills et al., 2016). We consider chemical absorption with an aqueous solution of monoethanolamine (MEA) as a solvent, since it is the most mature technology and has been considered in various benchmark studies of CO_2 capture processes (Voldsund et al., 2018b). The MEA absorption process we consider is shown in Fig. 4, and is adapted from the process flowsheets of Voldsund et al. (2019) and Ding et al. (2023). Here, the flue gases are cooled in a direct contact cooler and sent to an absorption column. In the absorption column, a solution of MEA (30% w/w) is brought in contact with the flue gases to absorb CO_2. Fresh aqueous

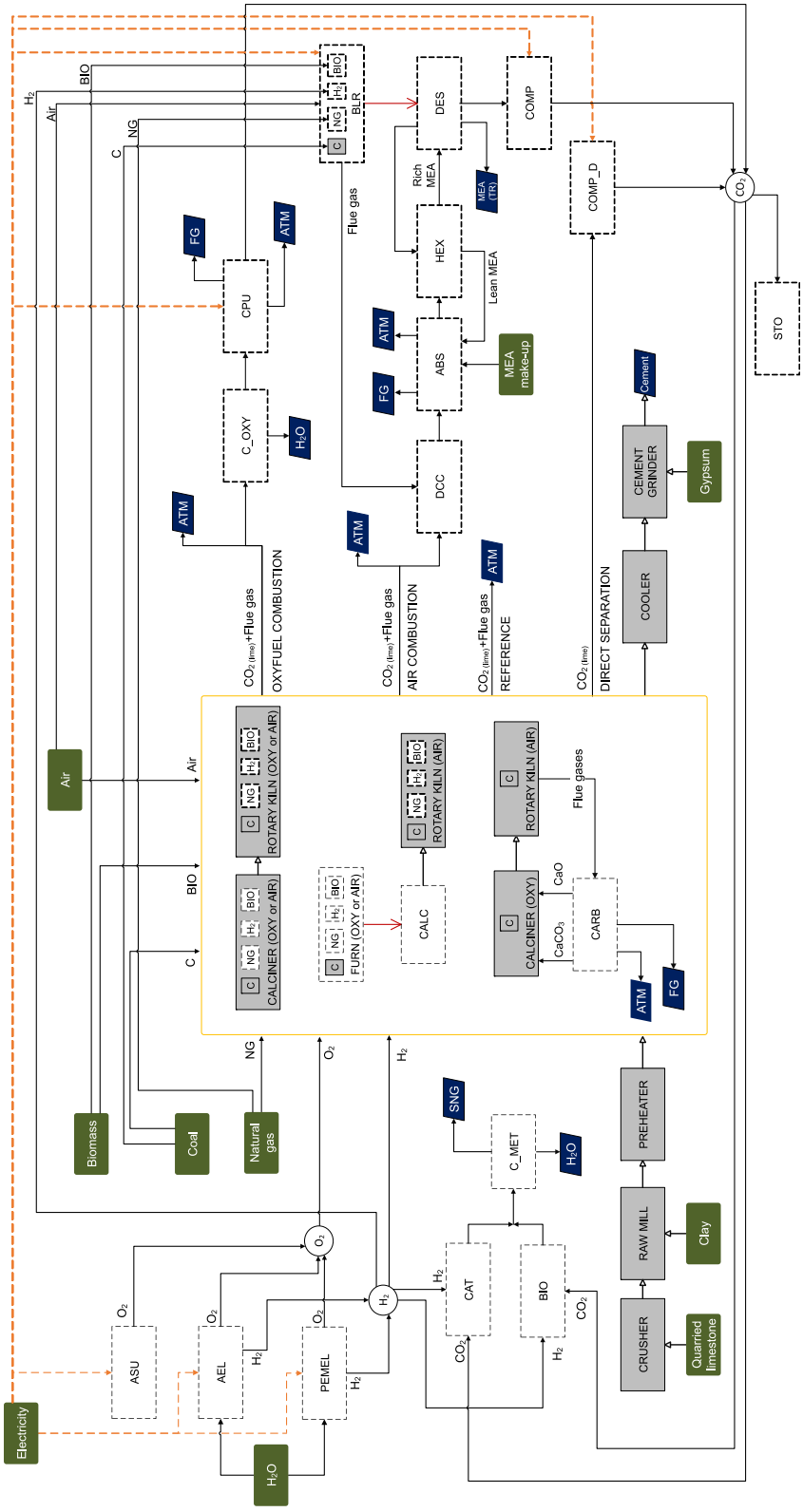

Fig. 3. Superstructure of retrofitted cement production. The units of the OPC production are represented by gray squares. Electricity flows are represented by orange dashed lines, heat flows by red solid lines and material flows by black solid lines. The calciner and kiln configuration are modified regarding the implemented retrofit technologies (white squares), e.g., for chemical absorption an existing calciner is used whereas for direct separation a new calciner is required. Oxygen required for oxyfuel combustion can be provided by an air separation unit or by water electrolysis. Captured CO_2 can be stored or utilized for producing SNG that is sold. We use the abbreviations: air separation unit (ASU), alkaline electrolyzer (AEL), polymer exchange membrane electrolyzer (PEMEL), catalytic reactor (CAT), biological reactor (BIO), condenser for methanation (C_MET), calciner (CALC), furnace (FURN), compressor for direct separation (COMP_D), carbonator (CARB), direct contact cooler (DCC), absorption column (ABS), liquid-liquid heat exchanger (HEX), desorption column (DES), boiler (BLR), compressor train (COMP), thermal reclaiming (TR), condenser for oxyfuel (C_OXY), carbon purification unit (CPU), CO_2 storage (STO), flue gases (FG), CO_2 emissions to atmosphere (ATM). For better readability, the sinks "ATM", "FG" and "H_2O" are represented as several sinks, although in the model they constitute single sinks.

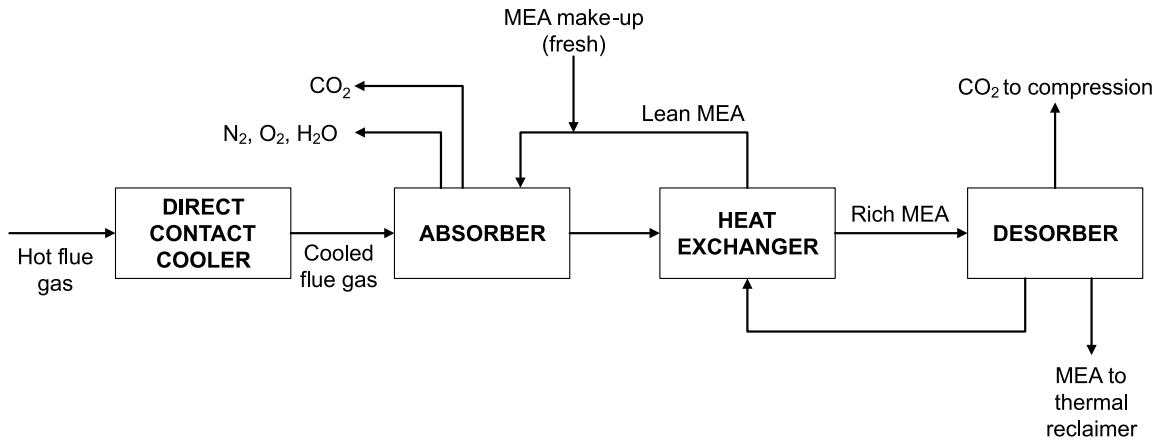

Fig. 4. Schematic diagram of chemical absorption process using MEA as solvent to capture CO_2 based on Voldsund et al. (2019) and Ding et al. (2023).

Table 2
Chemical absorption parameters.

Parameter	Value	Unit	Reference
MEA solvent requirement	4.677	kg_{MEA}/t_{CO_2}	Roussanaly et al. (2017)
Steam requirement	3.79	MJ/kg_{CO_2}	Roussanaly et al. (2017)
Absorber efficiency	90	%	Rao et al. (2004)
Compression power	0.314	MJ/kg_{CO_2}	Roussanaly et al. (2017)

Table 3
Oxyfuel combustion parameters.

Parameter	Value	Unit	Reference
Flue gas recycling fraction	55	%	[a]
CO_2 purification unit efficiency	90	%	[b]
CO_2 purification unit power consumption	122.2	kWh/t_{CO_2}	[c]
Air separation unit power consumption	226	kWh/t_{O_2}	[c]

[a] International Energy Agency-Greenhouse Gas R&D Programme (IEA-GHG) (2013).
[b] ECRA (2009).
[c] Voldsund et al. (2018a).

MEA solution (MEA make-up), a primary variable operating costs of MEA absorption technology, is continuously fed into the absorption column together with recycled CO_2 lean MEA solution (lean MEA) to compensate for losses due to evaporation and degradation during the absorption process. The remaining gases are released into the atmosphere, and the CO_2 rich MEA solution (rich MEA) passes through a liquid-liquid heat exchanger before being regenerated in a desorption column. Subsequently, the rich MEA stream enters the desorber where the CO_2 is released. The lean MEA stream is retrieved and recycled back to the absorber because of its high costs (Yin et al., 2021). After that, the released CO_2 is sent to a compressor train for further processing. An amount of MEA solvent is removed for thermal reclaiming. This subprocess is not included in our model, similar to Voldsund et al. (2019). More details on thermal reclaiming can be found, e.g., in Knudsen et al. (2009) and Sexton et al. (2014).

The regeneration step requires the supply of heat, e.g., by low-pressure steam or hot oil (Zhang et al., 2014). Steam is commonly used as a heat source for the regeneration process in chemical absorption based CO_2 capture in power plants (Xu et al., 2014; Dutcher et al., 2015; Alie, 2004; Wang et al., 2018). Fire-tube boilers are typically used for the production of low-pressure steam using natural gas or oil (Smith, 2016). Electric boilers are also suitable for steam generation and comprise a high efficiency (95 to 99%) (Zuberi et al., 2022). Therefore, we assume that either an electric boiler or a fire-tube boiler, using coal, natural gas or hydrogen, can generate the required steam. Implementing MEA absorption requires the installation of major components, i.e., direct contact cooler (DCC), absorption column (ABS), heat exchanger (HEX), desorption column (DES), compressor train (COMP) and boiler (BLR), as well as the use of a MEA solution (30% w/w). Parameters for modeling MEA absorption are shown in Table 2.

2.2.2. Oxyfuel combustion

In oxyfuel combustion, pure oxygen instead of air is used for combustion, obtaining a high CO_2 concentration in the flue gas resulting in an easier CO_2 separation. Oxyfuel combustion can be applied to both new and existing cement kilns (ECRA, 2009). For retrofitting cement plants, the main process units can be kept unchanged, i.e., the preheating, the calciner, and the rotary kiln, and other units have to be modified, i.e., the clinker cooler must be adapted for gas recirculation (Voldsund et al., 2018a). Implementation of oxyfuel combustion does not require the use of additional chemicals, feedstocks or heat but the installation of an onsite air separation unit with a significant electricity demand. We assume that the investment cost resulting from the oxyfuel implementation only accounts for the installation of new equipment, i.e., costs resulting from equipment modifications are neglected due to a lack of data. Additional components to be installed are a condenser (C_OXY) for cooling the flue gas stream, an air separation unit (ASU) to supply O_2, a mixer for recycling a fraction of the flue gas stream, and a carbon purification unit (CPU) for further treatment of captured CO_2. Parameters for implementing oxyfuel combustion are shown in Table 3.

2.2.3. Calcium looping

In a cement plant, calcium looping technology can be implemented as an end-of-pipe configuration, i.e., an additional calciner is required for CO_2 capture, or as an integrated configuration that utilizes the existing calciner for CO_2 capture that however operates in oxyfuel combustion (Voldsund et al., 2019). Since an integrated configuration avoids the installation of a new calciner, the investment costs are expected to be lower compared to the end-of-pipe configuration. Therefore, we consider the integrated calcium looping configuration shown in Fig. 5, similar to Rodríguez and Abanades (2012) and Voldsund et al. (2019). Here, the raw meal enters the oxy-fired calciner, producing CaO and CO_2. The CO_2 from limestone calcination and the flue gas from fuel combustion from the calciner are purified for downstream applications such as carbon utilization or carbon storage. Subsequently, a fraction of CaO is sent to the rotary kiln for clinker production, and the remaining CaO reacts in the carbonator with the CO_2 from fuel combustion in the flue gas stream from the rotary kiln. The produced calcium carbonate, $CaCO_3$, is then fed back to the calciner in a loop, while the separated gases N_2, O_2 and H_2O are released into the atmosphere.

Implementing an integrated calcium looping configuration requires the installation of a carbonator (CARB) and additional units to operate the calciner in oxyfuel combustion mode, i.e., an air separation unit

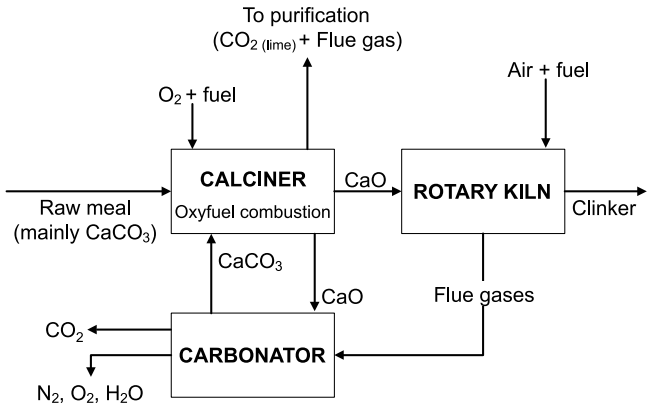

Fig. 5. Integrated calcium looping configuration for an operating cement plant based on Rodríguez and Abanades (2012) and Voldsund et al. (2019).

(ASU) and a mixer, and units to further treat the flue gases, i.e., a condenser (C_OXY), and a carbon purification unit (CPU). Similar to Voldsund et al. (2019), we assume a fixed CO_2 capture efficiency of 82% for the carbonator. The carbonator is formulated as an input–output model based on the fixed CO_2 capture efficiency, without modeling the reaction kinetics. In addition, we consider the parameters for oxyfuel combustion presented in Table 3.

2.2.4. Direct separation

Direct separation refers to separating the calcination and combustion reactions that occur in the calciner to capture CO_2 emissions from the limestone calcination. This technology uses indirect heating to calcine the limestone and obtain a pure CO_2 stream that is transported by a compressor for further use or storage (HeidelbergCement, 2020). Therefore, the calciner is the only unit that must be replaced for retrofitting a cement plant with direct separation, and no additional indirect costs are foreseen. However, the total degree of CO_2 capture is only around 60% due to the remaining emissions from fuel combustion (Driver et al., 2022). Thus, to achieve a higher degree of capture, we assume that the remaining emissions can be captured by a post-combustion carbon capture technology, i.e., chemical absorption (air combustion), or by a carbon purification unit (oxyfuel combustion). Alternatively, H_2 can be used to eliminate CO_2 emissions from combustion (Driver et al., 2022). Due to a lack of data on the investment cost of the indirect heating calciner, we model the direct separation as a combination of a fluidized bed reactor (CALC) and a furnace (FURN). The mass and energy flows for the calciner are calculated based on the mass and energy balance equations applied in the conventional calciner model. In addition, a compressor (COMP_D) is implemented to pressurize CO_2 from limestone calcination for transport.

2.2.5. Water electrolysis

Oxygen and hydrogen are produced from water and electricity in electrolysis. Three cell technologies have been developed for water electrolysis: alkaline (AEL), proton exchange membrane (PEMEL), and solid oxide (SOEL) (Holladay et al., 2009). AEL is the most mature and commonly used technology (Götz et al., 2016). PEMEL is considered an alternative technology for PtG projects due to its better capability for intermittent operation (Kopp et al., 2017). SOEL is still in development and requires higher temperatures and capital costs than AEL and PEMEL (Götz et al., 2016). Therefore, we consider AEL and PEMEL as two possible options in our superstructure. To determine the costs of installing an AEL or PEMEL system, we consider reference investment costs on 2018 of 1180 and 1640 EUR/kW_{el}, respectively (van Leeuwen and Zauner, 2018). The operational expenditures (OPEX) are assumed as 4% of the capital expenditures (CAPEX) for both types of systems, and an average efficiency, based on the lower heating value (LHV), of 67% for AEL and 64% for PEMEL (Buttler and Spliethoff, 2018).

2.2.6. CO_2 methanation

SNG is produced by combining captured CO_2 with H_2 from water electrolysis in a methanization step by catalytic or biological methanation (van Leeuwen and Zauner, 2018). Both technologies are considered promising. As of the 38 active methanization projects in 2019, half consider biological and half consider catalytic methanization (Thema et al., 2019). Thus, we include both technologies in our superstructure, both with an efficiency of 77.9% (van Leeuwen and Zauner, 2018). Pragmatically and following previous PtG studies (Chauvy et al., 2020; Delmelle and Heel, 2020), we assume that the SNG produced is purely CH_4 and has the properties of natural gas. We choose an average investment cost of 400 EUR/kW_{SNG} for catalytic methanation (CAT) and 550 EUR/kW_{SNG} for biological methanation (BIO), and the fixed OPEX are 10% of CAPEX for CAT and 5% for BIO (van Leeuwen and Zauner, 2018).

2.2.7. CO_2 storage

The application of CO_2 storage in cement industry has been globally studied in different projects (International Energy Agency-Greenhouse Gas R&D Programme (IEA-GHG), 2013). To decarbonize carbon-intensive industries, such as cement production, a CCS project between Germany and Norway is under development. Equinor and Wintershall Dea have announced a partnership to establish a large-scale value chain for CCS in the North Sea. The two companies intend to commission a 900-km open access pipeline by 2032, connecting a CO_2 collection hub in northern Germany to storage sites in Norway with an estimated annually capacity of 20 to 40 million tonnes of CO_2 (Wintershall Dea, 2022). The economic and environmental impact assessment of CO_2 storage strongly depends on the location and type of storage, e.g., geological or oceanic, the type of transport, e.g., pipeline or ship (Metz et al., 2005), and the transportation distance. We assume geological carbon storage, STO in Fig. 3, in the North Sea with an annual average capacity of 30 million tonnes of CO_2 and a pipeline transportation distance of 900 km based on the project of Wintershall Dea (2022). The cost and environmental effect of CO_2 storage are calculated in Section 1 of the supporting materials.

2.2.8. Sources and sinks

To evaluate the operational expenditures of retrofitting we account for the prices of electricity, fuels, and solvent, and, in case of sinks, a possible financial compensation or selling price. The sources in our superstructure that are relevant for calculating the operational expenditures are natural gas, coal, biomass, electricity, and MEA solvent. Natural gas and coal are considered to be purchased at large scale industrial consumer prices. For biomass, the quality of wood chips is secondary for large furnaces (>1 MW) (Kuptz and Hartmann, 2014) as using high-quality wood chips with low water content for a large-scale furnace would add unnecessary cost (Kuptz and Hartmann, 2014). According to information on the market price of wood chips in Germany (C.A.R.M.E.N.e.V., 2023), we consider wood chips with a water content of 35%. For the electricity supply we consider an average German day-ahead price plus an average grid fee (Bundesnetzagentur|SMARD.de, 2023; Bundesnetzagentur and Bundeskartellamt, 2023). Furthermore, the emissions to the atmosphere, the SNG by-product, and the cement main product constitute sinks in our model. For the cement sink, we fix a demand of 130 t/h, reflecting the production capacity of the reference process described in Section 2.1. For the process CO_2 emissions, from limestone calcination and fossil fuel combustion, we consider the need to purchase CO_2 certificates. For the SNG selling cost, the values reported in the literature vary from 0.05 EUR/kWh to 0.58 EUR/kWh (Vega Puga et al., 2022) and depend on the cost estimation method used and the assumptions considered for the production process, e.g., hydrogen production technology. In our study, we assume the market price of natural gas as the SNG selling price to obtain a conservative estimate of possible revenues from SNG production.

In the environmental impact assessment, we account for both direct emissions (CO_2 from the process) and indirect emissions (from the commodities). Specifically, we consider the upstream emission factors for the fuels, for the electricity, and for the solvent in chemical absorption. For electricity, we consider the emission factor based on the source of electricity generation. For biomass, we account for the upstream emissions from collecting, harvesting, chipping, and transportation of wood chips reported by Yang et al. (2022) but not the direct emissions from combustion. Moreover, the capture and storage of CO_2 from biomass combustion can lead to negative emissions. With respect to sinks, we consider direct CO_2 emissions arising from the process, i.e., limestone calcination and combustion, that are not captured. We also account for indirect emissions due to CO_2 storage from transport and injection (Koornneef et al., 2008). Finally, we assume that the sold SNG leads to avoided indirect GHG emissions, as it would replace natural gas. To assess the avoided GHG emissions, we consider the emissions from the German natural gas mix (Bundesnetzagentur and Bundeskartellamt, 2022). All economic and environmental calculations and parameter values can be found in Section 2 and in Tab. 1 of the supporting materials.

2.3. Process heat generation

Thermal energy is required in cement production to reach temperatures above 1400 °C in the rotary kiln to produce clinker (Fierro et al., 2020). Traditionally, coal and petcoke have been the main fuels in European cement production (Schorcht et al., 2013). According to the Global Cement and Concrete Association, in 2021, 80% of the fuel used for cement production globally consisted of fossil fuels, with the remaining fuel mix being comprised of biomass waste and alternative fuels such as industrial and non-industrial wastes (GCCA, 2021). Natural gas, biomass, and hydrogen have also been studied to reduce direct carbon emissions (El-Emam and Gabriel, 2021; Juangsa et al., 2022; Nhuchhen et al., 2021; Ozturk and Dincer, 2022; Walker et al., 2009). For instance, the US cement industry has used a mix of coal, petcoke, and natural gas (Smith, 2003).

Likewise, we consider a variety of fuels, i.e., hard coal, biomass, natural gas, and hydrogen in our superstructure. According to Grammelis et al. (2016), hard coal has a mass carbon content between 86 and 98%, and natural gas is predominantly methane. Hence, we model natural gas as pure methane and hard coal as pure carbon, see Tab. 6 of the supporting materials. With respect to biomass, we consider wood biomass from forestry and sawmill by-products, specifically wood chips, as they have been used for medium and large-scale biomass heat plant projects (BASIS, 2015) and in co-firing in a full-scale OPC production facility (Schindler et al., 2012). To model the combustion of wood chips, we assume that biomass can be abstracted as $CH_{1.44}O_{0.66}$ (Nussbaumer, 2003), see Tab. 6 of the supporting materials. Furthermore, we assume that the H_2 that is produced by PtH_2 can be used on site as a fuel for heat generation. We assume that the heat supply efficiency is 100% for all fuels. The lower heating values of the fuels can be found in the supporting materials in Section 4 and Tab. 7.

Due to the limited data available on kiln and calciner burner modifications required for the use of alternative fuels, we neglect the cost of retrofitting measures applied to these units. Similar to our previous study on hydrogen use in copper production (Röben et al., 2021), we assume that burners have to be replaced periodically and that such an occasion can be used to switch to an alternative burner technology.

3. Problem formulation

We formulate a superstructure model on the basis of linear mass and energy balances, nonlinear cost correlations, and further linear constraints. The model is implemented in our open-source energy system optimization framework COMANDO (Langiu et al., 2021). The nonlinear cost correlations are approximated as piece-wise linear functions by the automatic linearization in COMANDO which relies on the convex-combination method (Vielma et al., 2010). We have tried different numbers of linearization points and found that 10 points yield decent results. In preliminary testing, we solved the MINLP formulation using BARON 24.5.8 and we found that the MILP reformulation yields similar results compared to the MINLP solutions. Therefore, we opted for the MILP formulation to improve computational efficiency. The resulting mixed-integer linear program (MILP) has an economic and an environmental objective, i.e., the total annualized cost (TAC) of the energy- and emissions-related retrofitting measures and the global warming impact, respectively. We use the augmented epsilon constraint method (Mavrotas, 2009) to obtain Pareto-optimal plant designs with respect to TAC and GWI. The Pareto front is obtained by first independently minimizing the TAC and the GWI. The minimum-TAC and the minimum-GWI solutions define the end points of the Pareto front as well as the GWI range. Further Pareto-optimal designs are then computed by repeatedly minimizing the TAC with successively tightened constraints on the GWI. Specifically, six equidistant points in the GWI range are considered. The problem size of the superstructure MILP is 6641 equations, 6280 continuous variables and 11280 discrete variables. All MILPs are solved using Gurobi 9.5.1 (Gurobi Optimization, LLC, 2020) with a relative optimality tolerance of 1% on a desktop PC with an Intel i7-8700 processor and 32 GB RAM, running Windows 10 Enterprise LTSC.

3.1. Balance and constitutive equations

We model the cement production and retrofit technology units as input–output models, based on steady-state mass and energy balances. The set of components C is defined as $C = \mathcal{X} \cup \mathcal{L} \cup \mathcal{U} \cup \mathcal{A} \cup \mathcal{B} \cup \mathcal{H} \cup \mathcal{E} \cup \mathcal{O}$, with the set of mixers ($\mathcal{X}$), splitters ($\mathcal{L}$), conversion units ($\mathcal{U}$), combustors ($\mathcal{A}$), calciners ($\mathcal{B}$), thermal components ($\mathcal{H}$), electricity-based components ($\mathcal{E}$), and other components ($\mathcal{O}$).

Each component may have multiple mass and energy inputs and outputs. For a component c, the steady-state energy balance is represented by

$$\sum_i \dot{E}_{c,i}^{in} = \sum_j \dot{E}_{c,j}^{out}, \tag{1}$$

where $\dot{E}_{c,i}^{in}$ and $\dot{E}_{c,j}^{out}$ denote the entering and leaving energy flows, respectively, and i and j denote indices for enumerating the different flows. An output energy flow $\dot{E}_{c,j}^{out}$ may be related to an incoming energy flow $\dot{E}_{c,i}^{in}$ by

$$\dot{E}_{c,j}^{out} = \eta_{c,i\to j} \cdot \dot{E}_{c,i}^{in}, \tag{2}$$

using $\eta_{c,i\to j}$ as a known efficiency of conversion.

$\dot{S}_{el}$ denotes the electrical power demand of the process. It is determined by summing up the electrical power demands of the electricity-based components, i.e.,

$$\dot{S}_{el} = \sum_{c \in \mathcal{E}} \dot{E}_{c,el}^{in} \tag{3}$$

as the superstructure does not contain technologies for electricity production. The index el indicates that the energy flow $\dot{E}_{c,el}^{in}$ is an electric power demand.

We introduce a set $\mathcal{M}$ for the material sources (i.e., natural gas, coal, biomass, and MEA solvent) and a set $\mathcal{N}$ for the material sinks (i.e., SNG, cement, flue gases, water, biogenic CO_2 emissions, non-biogenic CO_2 emissions, stored biogenic CO_2 emissions, and stored non-biogenic CO_2 emissions). Then, the steady-state mass balance for a component c can be written as

$$\sum_{m \in \mathcal{M}} \dot{S}_{m,c} + \sum_i \dot{M}_{c,i}^{in} = \sum_j \dot{M}_{c,j}^{out}, + \sum_{n \in \mathcal{N}} \dot{S}_{n,c}, \tag{4}$$

distinguishing multiple input ($\dot{M}_{c,i}^{in}$) and output ($\dot{M}_{c,j}^{out}$) mass flows that originate from or leave to other components, respectively, as well as

mass flows that originate from sources ($\dot{S}_{m,c}$) and mass flows that leave to sinks ($\dot{S}_{n,c}$).

Mass flows may consist of multiple species. For instance, the mass flow $\dot{M}_{c,j,k}$ of a species k from the set of species $\mathcal{K}$ can be calculated by

$$\dot{M}_{c,j,k} = \dot{M}_{c,j} \cdot y_{c,j,k}, \tag{5}$$

where $y_{c,j,k}$ is the mass fraction.

For oxyfuel combustion, it is necessary to recirculate a certain amount of flue gas to maintain an appropriate flame temperature. The recycling loop includes a mixer and a splitter. A mixer x from the set of mixers $\mathcal{X}$ is modeled as

$$\dot{M}_x^{out} = \sum_i \dot{M}_{x,i}^{in}, \tag{6}$$

and a splitter l from the set of splitters $\mathcal{L}$ is described by the mass balance

$$\sum_j \dot{M}_{l,j}^{out} = \dot{M}_l^{in} \tag{7}$$

and the relations

$$\dot{M}_{l,j}^{out} = \zeta_{l,j} \cdot \dot{M}_l^{in} \tag{8}$$

using the known split fractions $\zeta_{l,j}$ that must add up to one.

Components where a chemical reaction occurs, i.e., fuel combustion, limestone calcination, water electrolysis, methanation, or carbonation, are modeled as a conversion unit $u \in \mathcal{U}$. For a conversion unit u, an entering or leaving mass flow may contain either a reactant $e \in \mathcal{E}_u$ or a product $g \in \mathcal{G}_u$, with $\mathcal{E}_u$ and $\mathcal{G}_u$ representing the set of reactants and products for the conversion unit u, respectively. We can assume complete reactions, i.e., full conversion of reactants; thus the mass flow of a generated product g in stream j is calculated as

$$\dot{M}_{u,j,g}^{out} = \dot{E}_{u,heat}^{out} \cdot \nu_{e,g,u} \cdot \left(\frac{w_g}{\Delta H_u} \right), \tag{9}$$

where $\nu_{e,g,u}$ is the stoichiometric ratio between the reactant e and the product g, w_g is the molecular weight of the product, ΔH_u is the heat of reaction, and $\dot{E}_{u,heat}^{out}$ is the heat produced by the amount of reaction taking place in the conversion unit u.

The set of thermal components $\mathcal{H}$ includes the condensers for SNG purification and CO_2 treatment from oxyfuel combustion and the heat exchanger for MEA absorption. For a heat exhanger h, the energy balance is derived based on the sensible heat as (Chen et al., 2022)

$$\dot{M}_{h,hot}^{in/out} \cdot c_{h,hot} \cdot \Delta T_{h,hot} = \dot{M}_{h,cold}^{in/out} \cdot c_{h,cold} \cdot \Delta T_{h,cold}, \tag{10}$$

where $\Delta T_{h,hot}$ and $\Delta T_{h,cold}$ represent the arithmetic temperature differences of the hot and cold side, respectively. The mass in- and outflows on any given side are identical, i.e., $\dot{M}_{h,hot}^{in/out} = \dot{M}_{h,hot}^{in} = \dot{M}_{h,hot}^{out}$ and $\dot{M}_{h,cold}^{in/out} = \dot{M}_{h,cold}^{in} = \dot{M}_{h,cold}^{out}$. Arithmetic mean temperatures on the respective hot and cold sides are used to compute the heat capacities $c_{h,hot}$ and $c_{h,cold}$.

In the case of a condenser h, a gaseous mixture containing water is cooled down. While the water condenses, the remaining components stay gaseous and form the residual gases. The energy balance considers the enthalpy in- and outflows as well as the removed heat:

$$\dot{E}_{(\text{gaseous mixture})}^{in} = \dot{E}_{(\text{residual gases})}^{out} + \dot{E}_{(\text{liquid water})}^{out} + \dot{E}_{heat}^{out} \tag{11}$$

The enthalpy flows $\dot{E}_{(\text{gaseous mixture})}^{in}$, $\dot{E}_{(\text{residual gases})}^{out}$, and $\dot{E}_{(\text{liquid water})}^{out}$ are calculated based on the respective mass flow, heat capacity, temperature, and aggregate state, so that Eq. (11) can be used to compute the removed heat $\dot{E}_{heat}^{out}$.

The nominal size of a component c is denoted by D_c^{nom}. It is restricted by a minimum and maximum size, D_c^{min} and D_c^{max}, respectively, and can be expressed in terms of mass or energy, e.g., mass for a mixer and energy for a furnace. Taking into account a binary decision variable x_c indicating whether the component c is installed or not, D_c^{nom} is constrained by

$$x_c D_c^{min} \leq D_c^{nom} \leq x_c D_c^{max}. \tag{12}$$

The bounds are chosen based on literature values. In case no data is available, we pragmatically assume that D_c^{min} is zero, and that there is no maximum size limit, i.e., a significantly large upper bound is given to the optimizer to avoid constraining the optimal solution. Tab. 2 of the supporting materials shows the chosen lower and upper bounds.

3.2. Economic model

The economic objective is the total annualized cost (TAC) of the retrofit. The TAC includes the energy-related and emission-related investment and operating costs, as well as the profits. The objective is defined as

$$TAC = \sum_{c \in C} (CX_c \cdot CRF + OX_c^{fix}) + \left(\sum_{s \in S} OX_s^{var} + OX_{CO_2}^{var} - R_{SNG} \right) \cdot 7920. \tag{13}$$

Here CX_c is the capital expenditure for component c, CRF is the capital recovery factor that transforms the investment cost into an annual cost, OX_c^{fix} represents the fixed operating expenditures, i.e., the maintenance cost, OX_s^{var} quantifies the variable operational expenditures from a commodity s of the set of commodities $S = \mathcal{M} \cup \{\dot{S}_{el}\}$, $OX_{CO_2}^{var}$ accounts for the expenditures from the payment of CO_2 certificates, and R_{SNG} constitutes the revenues from the SNG product. The variable operational costs and profits are calculated considering an operational period of 7920 h, i.e., 330 days.

The CAPEX CX_c from the installation of a component c are calculated based on economies of scale and expressed as a power law of capacity (Smith, 2016) as

$$CX_c = x_c \cdot CX_c^{ref} \cdot \left(\frac{D_c^{nom}}{D_c^{ref}} \right)^{\alpha} \cdot \left(\frac{CE^{2022}}{CE^{ref}} \right), \tag{14}$$

where the reference cost CX_c^{ref}, the reference size D_c^{ref}, and the scale factor α are taken from literature (Smith, 2016; Biegler et al., 1997) and can be found in Tab. 2 of the supporting materials. In addition, we use the Chemical Engineering Plant Cost Index (CEPCI) parameter CE^{2022}, published in February 2022 (Ma et al., 2023), and CE^{ref} to update the investment cost to the scenario year 2022, and currency exchange factors to convert the costs reported in USD to EUR. CEPCI parameters and currency exchange factors can be found in Tab. 4 and Tab. 5 of the supporting materials, respectively. CRF is calculated as (Lazou and Papatsoris, 2000)

$$CRF = \frac{(1+i)^n \cdot i}{(1+i)^n - 1}, \tag{15}$$

where n and i represent the project lifetime and the discount rate, respectively. The lifetime of cement kilns typically ranges from 30 to 50 years (Voldsund et al., 2019). Similar to other PtG and CCUS studies (Gorre et al., 2020; Global CCS Institute, 2021), we consider a project lifetime of 20 years. We assume a discount rate of 4.9% based on the weighted average cost of capital (WACC) for energy projects in 2020/21 (KPMG, 2021).

The fixed OPEX OX_c^{fix} are defined as

$$OX_c^{fix} = T_c^{fix} \cdot CX_c \quad \forall c \in C, \tag{16}$$

where the maintenance cost T_c^{fix} constitutes a fraction of the investment cost CX_c. The variable OPEX OX_s^{var} of a commodity s are calculated based on the consumption by

$$OX_s^{var} = p_s \cdot \dot{S}_s \quad \forall s \in S, \tag{17}$$

where p_s is the price of the commodity s and $\dot{S}_s$ is the quantity consumed. The operational expenditures for CO_2 emissions, $OX^{var}_{CO_2}$, are calculated by

$$OX^{var}_{CO_2} = p_{CO_2} \cdot \dot{S}_{CO_2}, \tag{18}$$

where p_{CO_2} is the price for CO_2 emissions certificates and $\dot{S}_{CO_2} \in \mathcal{N}$ is the amount of non-biogenic CO_2 emissions sent to the atmosphere. Revenues can be generated by selling the SNG product at a market price r_{SNG}, i.e.,

$$R_{SNG} = r_{SNG} \cdot \dot{S}_{SNG}, \tag{19}$$

with $\dot{S}_{SNG} \in \mathcal{N}$.

3.3. Environmental model

The environmental objective is the global warming impact (GWI) defined as

$$GWI = \Bigg(GWI^{dir} + \sum_{s \in S} GWI^{ind}_s + GWI^{ind}_{stoCO_2} + GWI_{SNG} - GWI^{ind}_{SNG} - CS_{bio} \Bigg) \cdot 7920. \tag{20}$$

Here, GWI^{dir} accounts for the GWI due to all non-biogenic direct CO_2 emissions that are released to the atmosphere (i.e., fossil-based CO_2 that is emitted rather than captured). These include process emissions from fossil fuel combustion and limestone calcination. GWI^{ind}_s quantifies the indirect impact from the use of commodities, $GWI^{ind}_{stoCO_2}$ accounts for the indirect impact associated with the transport, injection, and storage of CO_2. The term GWI_{SNG} represents the emissions attributed to the SNG produced from captured CO_2 from fossil sources. GWI^{ind}_{SNG} accounts for the indirect emissions of conventional natural gas production that are avoided by substituting conventional natural gas with SNG. Similar to other studies that consider the storage of biogenic CO_2, see, e.g., Yang et al. (2022) and Domingos et al. (2023), we introduce credits for the stored biogenic CO_2, i.e., CS_{bio}.

The direct GWI is quantified by

$$GWI^{dir} = \sum_{a \in \mathcal{A}} \sum_{f \in \mathcal{F}} EM_{f,a} + \sum_{b \in \mathcal{B}} EM_{lime,b} - CO^{capt}_2, \tag{21}$$

where CO^{capt}_2 denotes the captured CO_2 emissions for subsequent utilization or storage. $EM_{f,a}$ represents the CO_2 emissions related to the combustion of fuel f from the set $\mathcal{F}$ of fossil fuels, i.e., natural gas and coal, arising from a combustor a from the set of combustors $\mathcal{A}$. $EM_{lime,b}$ denotes the limestone calcination emissions from calciner b from the set of calciners $\mathcal{B}$. These are calculated as

$$EM_{f,a} = EF_f \cdot \dot{M}^{in}_{a,f}, \tag{22}$$

$$EM_{lime,b} = EF_{lime} \cdot \dot{M}^{in}_{b,lime}, \tag{23}$$

with EF_f and EF_{lime} representing the CO_2 emission factors that can be found in Tab. 1 of the supporting materials. $\dot{M}^{in}_{a,f}$ represents the fuel consumption of the combustor a and $\dot{M}^{in}_{b,lime}$ is the limestone mass flow entering calciner b.

The indirect GWI from the use of commodities is calculated as

$$GWI^{ind}_s = EF^{ind}_s \cdot \dot{S}_s, \tag{24}$$

where EF^{ind}_s is the emission factor from a commodity s and $\dot{S}_s$ is the consumed amount. Upstream emission factors from commodities can be found in Tab. 1 of the supporting materials.

Indirect emissions arising from the storage of CO_2 are calculated as

$$GWI^{ind}_{stoCO_2} = EF^{ind}_{sto} \cdot \dot{S}_{stoCO_2}, \tag{25}$$

where EF^{ind}_{sto} is the emission factor of CO_2 storage, see Section 1 of the supporting materials, and $\dot{S}_{stoCO_2}$ represents the stored non-biogenic or biogenic CO_2.

In accordance with the methodology suggested in Abanades et al. (2017), we assume that, if the CO_2 used in the synthesis of SNG originates from fossil sources, the maximum theoretical emissions mitigation potential is 50%. The emissions attributed to the SNG produced from fossil carbon thus is calculated as

$$GWI_{SNG} = (1 - f_{SNG}) \cdot EF_{SNG} \cdot \dot{S}^{fos}_{SNG}, \quad \text{with } f_{SNG} = 0.5, \tag{26}$$

where EF_{SNG} is the emission factor for SNG combustion, see Tab. 1 of the supporting materials, and $\dot{S}^{fos}_{SNG}$ is the amount of SNG produced from fossil carbon sources and sold to the market.

The avoided indirect emissions of natural gas production are computed as

$$GWI^{ind}_{SNG} = EF^{ind}_{SNG} \cdot \dot{S}_{SNG}, \tag{27}$$

where EF^{ind}_{SNG} is the emission factor from imported natural gas production used in Germany, see Section 2 and Tab. 1 of the supporting materials, as we assume that the produced SNG, i.e., $\dot{S}_{SNG}$, replaces natural gas in the market.

Finally, credits from storage of biogenic CO_2 are calculated as

$$CS_{bio} = \dot{S}_{bCO_2}, \tag{28}$$

where $\dot{S}_{bCO_2}$ is the stored biogenic carbon dioxide.

4. Results and discussion

We now present the optimal designs for retrofitted OPC production plants by focusing on the trade-offs between the energy- and emission-related TAC (see Eq. (14)) and the GWI (see Eq. (20)). In addition, we analyze the influence of selected model parameters on the obtained optimal designs as part of a sensitivity study.

4.1. Scenario description

We distinguish eight scenarios based on the availability of sufficient amounts of biomass, the availability of CO_2 storage, and the assumed emission factor of the electricity mix (see Table 4). The later is a critical parameter due to the power intensity of various technologies in the superstructure. From a technological perspective, using biomass as a fuel is a viable option to reduce CO_2 emissions (Ige et al., 2024), although uncertainties remain about its availability as a bioenergy source (Jering et al., 2013). Likewise, utilization of CO_2 storage (STO in Fig. 3) can significantly reduce CO_2 emissions of cement production (Barbhuiya et al., 2024; Anderson and Newell, 2004). However, CO_2 storage is subject to uncertainties related to economics, transportation, and available storage volumes (Purr et al., 2023).

For scenarios 1–4 (Table 4), we consider a high electricity GWI based on the German electricity mix in 2022, where coal accounted for 33% of electricity generation, resulting in an annual emission factor of 434 g $CO_{2_{eq}}$/kWh (Icha and Lauf, 2022). In contrast, scenarios 5–8 consider a low emission factor based on Norway's electricity mix in 2020, where 92% of electricity generation was from renewable sources, leading to an annual emission factor of only 10 g $CO_{2_{eq}}$/kWh (International Energy Agency (IEA), 2022). In the scenarios with biomass, we assume wood chips with a cost of 101.76 EUR/t (C.A.R.M.E.N.e.V., 2023) as the source of bioenergy. In scenarios without biomass, we restrict the fuel set in the superstructure to coal, natural gas, and hydrogen. For scenarios that include CO_2 storage, the storage cost is set to 35.56 EUR/t CO_2, based on our own calculations that assume an average storage capacity of 30 Mt CO_2/y and a pipeline distance of 900 km based on the initiative of Wintershall Dea (2022). The detailed CO_2 cost calculations can be found in Section 1 of the supporting materials.

Table 4
Scenarios differ with respect to availability of CO_2 storage and biomass and the emission factor of the electricity mix.

Scenario (Sc)	CO_2 storage availability	Biomass availability	Emission factor of electricity mix
1	×	×	434 g CO_{2eq}/kWh
2	×	✓	434 g CO_{2eq}/kWh
3	✓	×	434 g CO_{2eq}/kWh
4	✓	✓	434 g CO_{2eq}/kWh
5	×	×	10 g CO_{2eq}/kWh
6	×	✓	10 g CO_{2eq}/kWh
7	✓	×	10 g CO_{2eq}/kWh
8	✓	✓	10 g CO_{2eq}/kWh

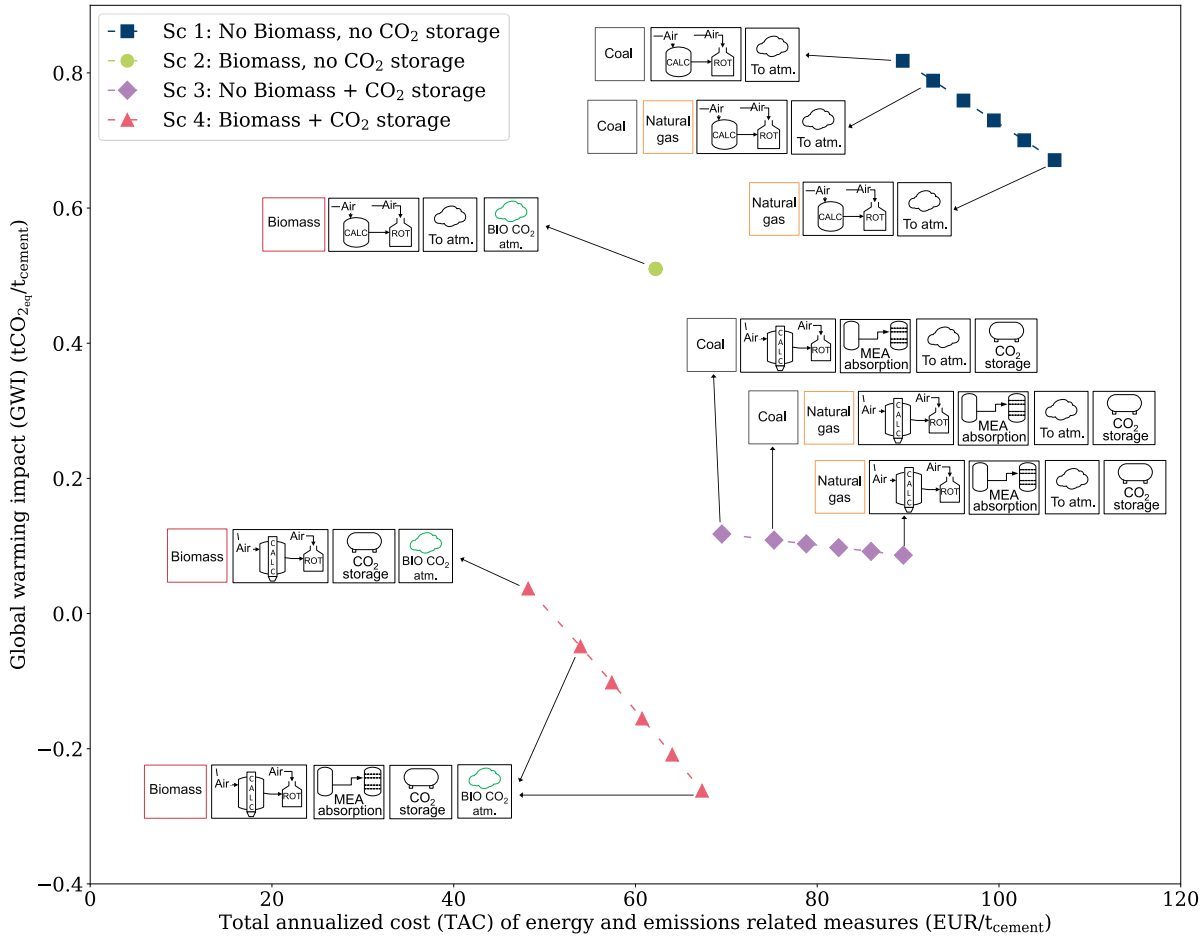

Fig. 6. Pareto-fronts for the high-GWI scenarios. The technologies installed and the fuels selected are depicted for selected Pareto-optimal designs. For the Pareto-optimal designs for which no process configuration is depicted, the design remains the same as in the preceding design on the respective curve (read from left to right), with the only difference being the amount of CO_2 that is captured.

4.2. Optimal designs for high-GWI electricity mix

Fig. 6 shows the Pareto fronts for the scenarios with a high emission factor of the electricity mix (scenarios 1–4). The interpolated lines between the optimal designs are added to guide the eye of the reader. The markers show the Pareto-optimal designs. Pareto optimality means that a further improvement in one objective cannot be achieved without worsening with respect to the other objective (Luc, 2008). Thus, the Pareto front represents the trade-off between the economic and the environmental objective. For each Pareto front, except the one for Scenario 2, six different Pareto-optimal designs are computed. In Scenario 2, the Pareto front is composed of a single point, indicating that there exists no trade-off between the two objectives. The partly linear appearance of the Pareto curves can be explained by the fact that the respective designs only differ regarding the fuel mix and the amount of captured CO_2.

Unavailability of biomass as an energy source (Scenarios 1 and 3) leads to the selection of hard coal or natural gas as fuels. For Scenario 1, the GWI can only be reduced by replacing parts or all of the hard coal with natural gas. Therefore, the optimal design of Scenario 1 considers the process units of the reference plant only (Section 2.1) and opts for the payment of CO_2 certificates.

In Scenario 2 (biomass is available but carbon storage is not) the optimal design uses biomass as a cheaper and environmentally friendlier fuel than coal and natural gas. Specifically, replacing hard coal (first Pareto point in Scenario 1) with biomass (Scenario 2) reduces both the GWI and the TAC by more than 30%. Note that the CO_2 emitted from biomass combustion is part of the biogenic carbon cycle and thus exempt from the payment of CO_2 certificates.

Our finding of biomass being both economically and environmentally preferred agrees with Beguedou et al. (2023), who highlight the use of biomass in the cement industry to reduce both the GWI and the

energy expenditures. In Europe, biomass has partially replaced fossil fuels for heat supply in the cement industry (Favier et al., 2018). From a technical perspective, high substitution rates are possible, potentially reaching 100% replacement with waste and biomass fuels (Marmier, 2023), provided there is sufficient access to and continuous availability of biomass (CEMBUREAU The European Cement Association, 2020; Luo et al., 2024).

Scenarios 3 and 4 demonstrate that the implementation of CO_2 storage, direct separation, and MEA absorption technologies can significantly reduce the GWI, even to negative values. In Scenario 3, the cost-optimal solution, i.e., the left Pareto point, shows a 86.7% decrease in GWI compared to the cost-optimal design of Scenario 1, i.e., the BAT plant (see Fig. 2), mainly due to the implementation of CO_2 storage. The BAT plant represents the non-decarbonized system, i.e., no renewable or low carbon fuel and no carbon capture technologies are selected. Furthermore, as we consider the average price in 2023 for CO_2 emission certificates of 83.53 EUR/t CO_2 (EEX, 2023), the optimizer prefers CO_2 storage, with a calculated cost of 35.56 EUR/t CO_2, over paying for certificates. This preference results in a 22% reduction in the TAC compared to the BAT plant. Scenario 4 also shows the potential of achieving negative emissions by combining CO_2 storage and use of biomass as a fuel. Specifically, the most negative GWI, i.e., −0.26 t $CO_{2_{eq}}$/t cement (indicated by the right most design of Scenario 4 in Fig. 6), is achieved by fully capturing the CO_2 emissions from limestone calcination by direct separation technology. Additionally, 90% of the biomass combustion emissions are captured using MEA absorption technology and then stored.

Storing CO_2 (Scenarios 3 and 4) and replacing coal with a less carbon-intensive (natural gas in Scenarios 1 and 4) or carbon-neutral (biomass in Scenarios 2 and 4) fuel are the optimal options to reduce the overall emissions. CO_2 utilization, i.e., SNG production, is inferior and thus not part of the optimal designs. This can be explained by the fact that the hydrogen required for SNG production is generated via electrolysis (AEL or PEMEL), which would become highly carbon-intensive with the assumed high electricity emission factor.

4.3. Optimal designs for Norway electricity mix

The Pareto fronts for scenarios 5–8, which consider an electricity GWI of only 10 g $CO_{2_{eq}}$/kWh, are shown in Fig. 7. The Pareto curve in Scenario 5 has a partly linear appearance. The respective designs only differ with respect to the amount of captured CO_2, but do not comprise different capture technologies. The almost linear nature of the Pareto curve for Scenario 6 can be attributed to (i) changes in the amount of captured CO_2 and (ii) MEA and oxyfuel technologies causing very similar cost and GWI.

Considering the low emission intensity of the electricity mix, the low-GWI designs of scenarios 5 and 6 include CCU technologies to take advantage of the emission mitigation potential of CCU systems. In scenarios where CO_2 storage is unavailable (Scenarios 5 and 6), the CCU technologies are crucial for reducing the GWI. They however come at very high costs. Oxyfuel combustion and SNG production from partial capture of limestone calcination emissions achieve GWI reductions of 40.6% and 19.8%, corresponding to the fourth and third Pareto solutions from the left in Scenarios 5 and 6, respectively. In Scenarios 5 and 7 (no biomass), hard coal is preferred as a fuel in the minimum-TAC design, while hydrogen produced via AEL is preferred in the minimum-GWI design.

Implementing CO_2 storage achieves very low GWI values of 0.02 and −0.3 t $CO_{2_{eq}}$/t cement in Scenarios 7 and 8, at comparatively low TAC of 172 and 67 EUR/t cement, respectively. If carbon storage is not available, the highest GWI reduction, to 0.26 t $CO_{2_{eq}}$/t cement, is achieved by a combination of CCU technologies and hydrogen as a fuel, however at extreme costs of 680 EUR/t cement (Scenario 5) and 555 EUR/t cement (Scenario 6).

It can be noted that in the low-electricity-GWI scenarios, a wider variety of technologies is implemented and that GWI and TAC vary more significantly than in the high-electricity-GWI scenarios. With the low-GWI electricity mix being considered more representative for the future, we analyze in detail the optimal capacities, CO_2 emissions, and cost structures of the low-electricity-GWI scenarios.

4.3.1. Capacities of the Pareto-optimal designs

Fig. 8 shows the optimal capacities of the selected technologies for retrofitting the OPC production process across the low-electricity-GWI scenarios 5 to 8.

The cost-optimal design for Scenario 5 is the BAT plant, while for Scenario 6 only coal is replaced by biomass, thus no retrofit technology capacities are included. In contrast, for the mininum-TAC designs in Scenarios 7 and 8, direct separation (Scenarios 7 and 8), MEA absorption (Scenario 7), and CO_2 storage (Scenarios 7 and 8) are needed. Note that the CCS capacity is 33% higher in Scenario 7, compared to Scenario 8, as the latter scenario considers biomass as fuel and thus only requires storage of CO_2 emissions from limestone calcination.

For the GWI-optimal designs in Scenarios 5 and 6, PtMe and PtH_2 technologies are implemented, as CO_2 emissions from limestone calcination can be captured and utilized to produce SNG. As expected, the AEL unit is by far the largest consumer of electricity, reaching capacities of 0.52 GW (Scenario 5) and 0.43 GW (Scenario 6), surpassing the electricity consumption of other units, such as compressors.

In scenarios implementing CCS technologies, electricity demand reaches 0.1 GW and 0.055 GW in Scenarios 7 and 8, respectively. In Scenario 7, the AEL unit accounts for approximately 93% of the total electricity consumption, whereas in Scenario 8, the main electrical units are the electric boiler and the compressors. We observe that the capacities of carbon capture and carbon storage technologies increase along the Pareto fronts from minimum TAC to minimum GWI, leading to gradual reductions in emissions in all scenarios, except for Scenario 7. In Scenario 7, the GWI decrease is achieved by replacing carbon-intensive fuels with cleaner options like hydrogen, which decreases CO_2 emissions and thus allows for smaller capture and storage equipment. For instance, CCS capacity drops from about 97.88 to 65.8 t CO_2/h, from the minimum-TAC design to the minimum-GWI design. Conversely, a gradual increase in the use of CO_2 storage can be observed for Scenario 8, where a peak of 108 t CO_2/h (sixth Pareto-optimal design) is reached by capturing emissions from biomass combustion and limestone calcination. These trends highlight the distinct strategies needed to achieve GWI reductions and the increased CO_2 storage demands if biomass shall be used as fuel.

4.3.2. CO_2 emissions structure of the pareto-optimal designs

Fig. 9 shows the distribution of CO_2 emissions for the Pareto-optimal designs of scenarios 5–8. Direct emissions contributing to the GWI arise from fossil fuel combustion or limestone calcination, whereas indirect emissions are associated with fuel use, CO_2 storage, MEA solvent use, and electricity use.

Retrofitting OPC production with CCU or CCS technologies results in indirect emissions, which however are considerably lower than the direct emissions from limestone calcination and fuel combustion. Although the overall indirect emissions are quite low, a large part of them arise from the use of electricity. Unsurprisingly, CO_2 emitted to the atmosphere reaches its highest value if CO_2 storage and biomass are not available.

If CO_2 storage is available, CO_2 emissions from limestone calcination to the atmosphere are avoided, with the only remaining direct CO_2 emissions stemming from the combustion of fossil fuels (Scenario 7) or biomass (Scenario 8). If biogenic CO_2 is stored, negative emissions and thus credits can be attained. The maximum possible amount of biogenic CO_2 captured, however, is 334 kt CO_2, with the remaining 37 kt CO_2 being emitted to the atmosphere, due to the assumed capture rate of 90% for the carbon capture technologies. In scenarios where biomass

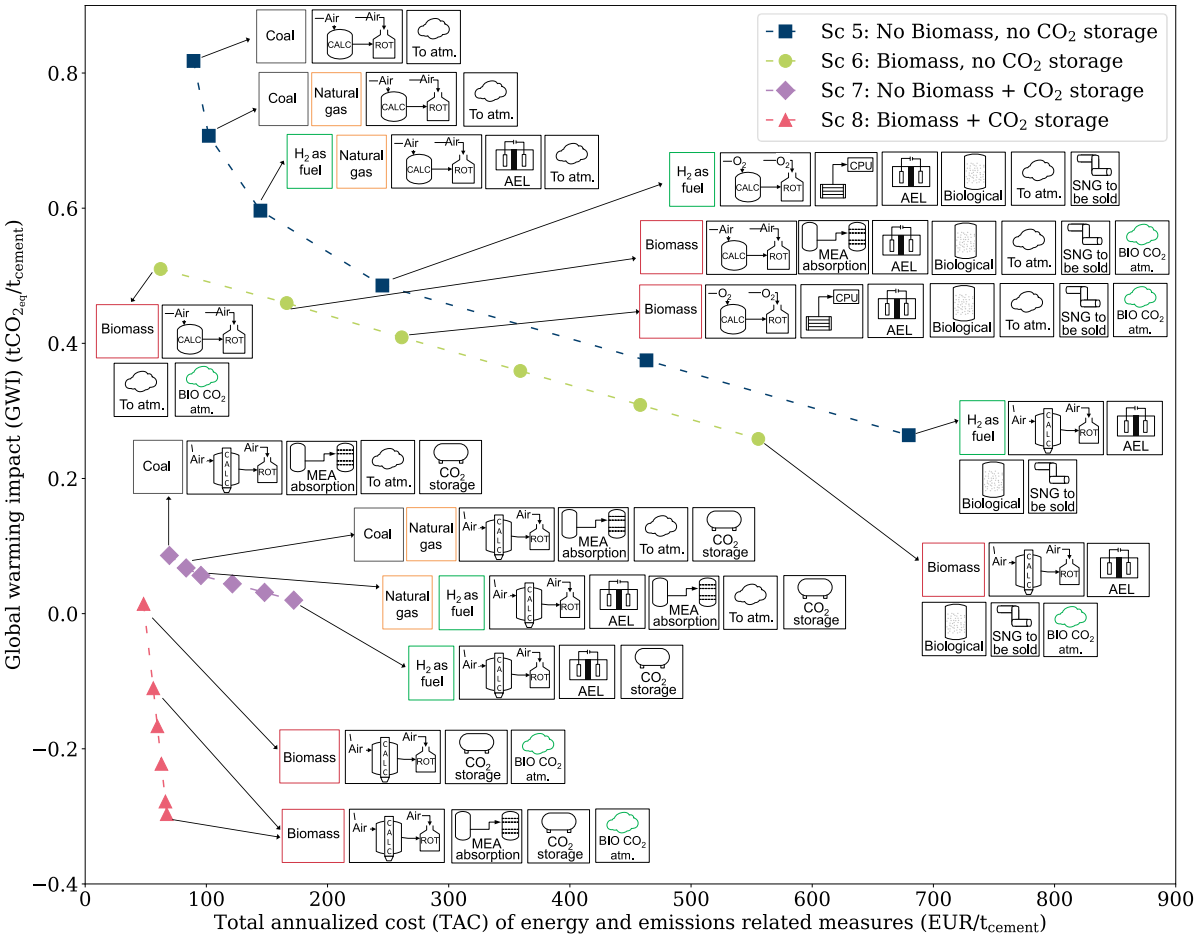

Fig. 7. Pareto-fronts for low-GWI scenarios. The technologies installed and the fuels selected are depicted for selected Pareto-optimal designs. For the Pareto-optimal designs for which no process configuration is depicted, the design remains the same as in the preceding design on the curve (read from left to right), with the only difference being the amount of CO_2 that is captured.

storage is not available, a carbon-negative design is not feasible. If CCU technologies are implemented, direct emissions from fossil sources are reduced, however, indirect emissions from electricity use remain and the avoided indirect emissions of natural gas production, from SNG sales, are not sufficient to offset them.

4.3.3. Costs structure of the Pareto-optimal designs

The analysis of the TAC components in Fig. 7 shows how the distribution of costs vary based on the system configuration and the scenario parameters, i.e., the availability and unavailability of biomass and CO_2 storage. The breakdown of the TAC includes the energy-related and emission-related OPEX and CAPEX.

The TAC of the Pareto-optimal designs are dominated by OPEX, irrespective of whether carbon storage or utilization technologies are implemented (see Fig. 10). Most of the operating costs arise from fuel purchase and CO_2 storage, if CCS is implemented, while electricity costs dominate if optimal designs rely on CCU technologies. Capturing CO_2 by chemical absorption results in the purchase of MEA solvent; however, solvent costs are very low, less than 2 EUR/t cement.

In general, CAPEX are very low for designs that consider CO_2 storage. They strongly rise, if CCU technologies are implemented, due to the high costs for AEL and PtMe technologies. For instance, in case of the minimal-GWI design in Scenario 5, the AEL unit and the methanation reactor are the major drivers of CAPEX, with 71.9% and 21.8%, respectively. Still, CAPEX remain well below 20% of TAC in all optimal designs and in all scenarios.

In the power-intensive designs, electricity costs dominate all other costs. High electricity costs are mainly due to the hydrogen production via AEL and the average electricity price of 128 EUR/MWh considered in the analysis. Thus, for minimal-GWI designs, except in Scenario 8, nearly all operational costs arise from electricity and account for more than 80% of TAC.

The revenue that can be obtained from the sale of SNG is generally insufficient to offset the electricity costs. For instance, in Scenarios 5 and 6, 198.29 EUR/t cement of SNG revenue is obtained, with 765.28 EUR/t cement of expenses arising from electricity purchases. Thus, only a heavy price premium that would make SNG more than three times as expensive as natural gas could offset the electricity costs.

4.4. Sensitivity analysis: Impact of electricity cost, CO_2 storage cost and biomass availability

The cost breakdown largely attributes the TAC to the operating costs, whereby the electricity costs for the CCU technologies stand out. However, electricity prices vary considerably depending on factors such as geography (Vereinigung der Bayerischen Wirtschaft (vbw), 2023) or the share of renewables in the generation mix (Kolb et al., 2020; Cevik and Ninomiya, 2023).

The sensitivity analysis by Gardarsdottir et al. (2019) shows that higher electricity prices lead to higher CO_2 avoidance costs for electricity intensive carbon capture technologies (such as oxyfuel combustion). On the other hand, Kenkel et al. (2021) show that lower electricity prices result in lower overall net production costs for carbon utilization technologies. Based on the electricity prices ranges provided in Gardarsdottir et al. (2019) and Kenkel et al. (2021), we study how lower

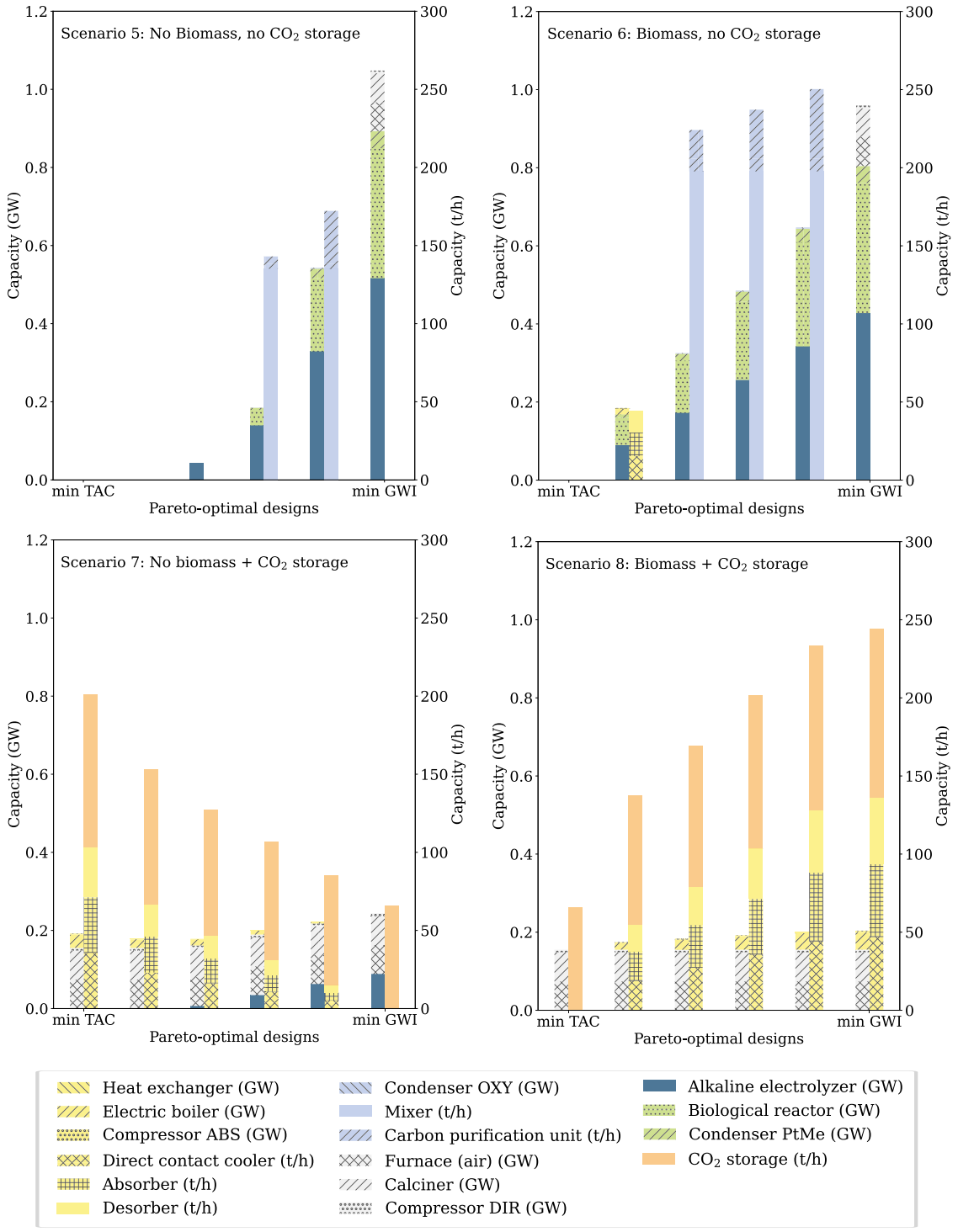

Fig. 8. Capacities of technologies in the Pareto-optimal designs for scenarios 5–8. The left y-axis represents the capacity in GW (electricity or heat), while the right y-axis indicates the capacity in tonnes per hour (t/h), e.g., tonnes of CO_2. With regard to minimum TAC in Scenarios 5 and 6, the BAT plant design is optimal, which does not contain any retrofit technologies. Process units are color-coded based on the employed technology: yellow (MEA absorption), light blue (oxyfuel combustion), gray (direct separation), light green (PtMe), blue (PtH_2), and orange (CO_2 storage).

electricity prices, i.e., 60 EUR/MWh and 20 EUR/MWh, affect the obtained Pareto-optimal designs.

Unsurprisingly, the Pareto fronts move from the right to the left with decreasing electricity prices (Fig. 11), i.e., for a given GWI, lower electricity prices reduce the TAC. For a minimum-GWI design, for instance, the TAC decreases by more than 50% and 90% compared to the reference value, for electricity prices of 60 and 20 EUR/MWh, respectively.

The very low electricity price of 20 EUR/MWh shrinks the Pareto fronts and moves them to the lower left corner. The resulting optimal designs show very little TAC variation for Scenario 5. Scenario 6 shows a single solution, indicating no trade-off between the two objectives. Here, CCU technologies are more cost-effective than the payment for CO_2 certificates. In fact, the cost-optimal solution does no longer exclusively rely on the payment of CO_2 certificates. In Scenario 6, only CCU technologies are implemented, whereas in Scenario 5, due to the

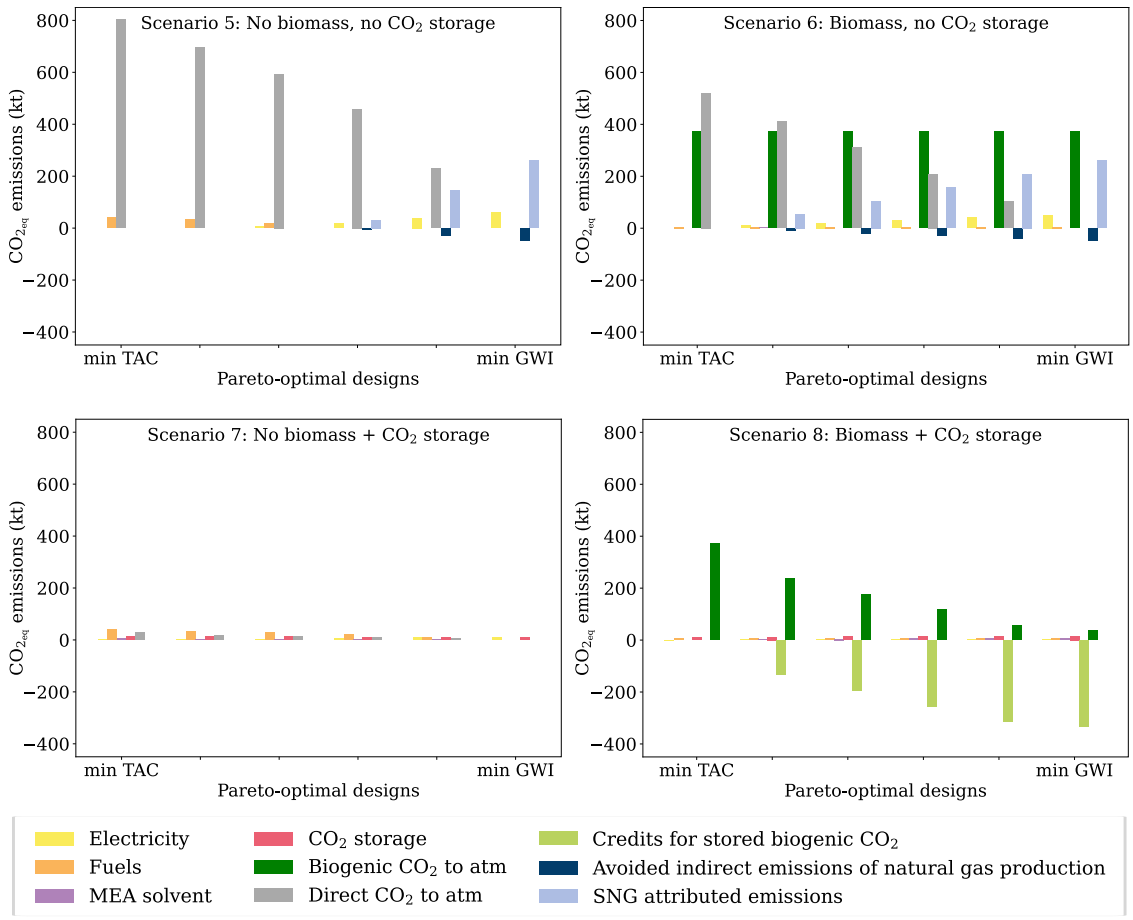

Fig. 9. CO_2 emission breakdown of the Pareto-optimal designs for scenarios 5–8. Indirect emissions from fuel production (orange bars) consider coal, natural gas and biomass. Emissions from CO_2 storage (red bars) include indirect emissions from transport and injection of CO_2 into geological storage. Direct CO_2 emissions to the atmosphere (gray bars) come from limestone calcination and combustion of fossil fuels, i.e., coal and natural gas. Biogenic CO_2 to atm represents CO_2 emissions from biomass combustion that are not stored or utilized. SNG attributed emissions (light blue bars) are calculated as described in Section 3.3. Avoided indirect emissions of natural gas production (blue bars) are obtained from the sale of SNG (replacing natural gas on the market). Negative emissions can be achieved from the storage of biogenic CO_2 (light green bars).

assumed capture rate of 90%, the remaining emissions from fossil fuel combustion are tackled by a combination of paying for CO_2 certificates and installing CCU technologies. In contrast, for electricity prices of 60 and 128 EUR/MWh, three types of designs emerge: (i) those that solely rely on payment for CO_2 certificates, (ii) those that comprise a combination of paying for CO_2 certificates and implementing CCU technologies, and (iii) those that exclusively use CCU technologies.

CO_2 storage cost estimates in the literature vary considerably and depend on the field characteristics such as type (new or reused wells), location (onshore or offshore) or geophysical condition (field depth) (ZEP, 2011). For instance, the Intergovernmental Panel on Climate Change (IPCC) (2014) stated that an uniform cost of \$10/t CO_2 would be a reasonable assumption for CCS deployment scenarios. In contrast, Smith et al. (2021) calculate onshore pipeline transport and storage costs ranging from 4 to 45 EUR/t CO_2, and 30 to 55 EUR/t CO_2 for offshore storage and shipping transport. Furthermore, an interactive tool from the Clean Air Task Force (CATF) (2023) provides an overview of CO_2 transport and storage costs in Europe ranging from 15 to 175 EUR/t CO_2. In the light of this considerable uncertainty, we investigate the effects of different assumed CO_2 storage costs. Specifically, we compute the Pareto fronts for Scenarios 7 and 8 (availability of CO_2 storage) for three different storage costs: 175 EUR/t CO_2, 115 EUR/t CO_2, and 35 EUR/t CO_2 (Fig. 12).

Fig. 12 shows that the use of CO_2 storage gives rise to an L-shaped Pareto curve in some cases in Scenario 7, i.e., starting from a minimal-TAC design, the GWI can be reduced drastically with rather small increases in the TAC. Thus, even for storage costs as high as 175 EUR/t CO_2, CO_2 storage remains the preferred option compared to CCU technologies

In Scenario 7, the kink of the L-shaped Pareto curves shows the transition from fossil fuels (natural gas) to renewables (hydrogen from AEL), resulting in an increase of more than 40% in the TAC from the fifth Pareto-optimal design to the minimum-GWI design. In Scenario 8, biomass is the preferred fuel, and the minimum GWI is only achieved by the total capture of CO_2 from both limestone calcination and biogenic sources, even in Pareto-optimal designs where storage costs of 115 and 175 EUR/tCO_2 are assumed. Furthermore, as expected, for CO_2 storage costs above the assumed CO_2 certificate price of 83.53 EUR/t CO_2, the optimal designs prefer emitting the CO_2 instead of storing it for achieving the minimum TAC. However, certificates prices are expected to increase in the future, e.g., they are predicted to reach values between 130 to 160 EUR/t CO_2 in 2030 (Pahle et al., 2022) and 310 EUR/t CO_2 in 2050 (EU Commission, 2011).

Local availability of biomass is an important factor for its use as fuel in cement production (International Energy Agency (IEA) Bioenergy, 2021). Local biomass supply avoids long-distance road transport, which can significantly increase transportation costs (Möller and Nielsen, 2007). To study the sensitivity of the system to limited biomass availability, we consider scenarios in which only a fraction of the required biomass can be supplied. Here, we take as a reference case (100% availability) the amount of biomass utilized in Scenarios 6 and 8, i.e., 25.6 t/h. We consider reduced availability levels of 60%, 30%, and 0% relative to this reference. We evaluate how varying degrees

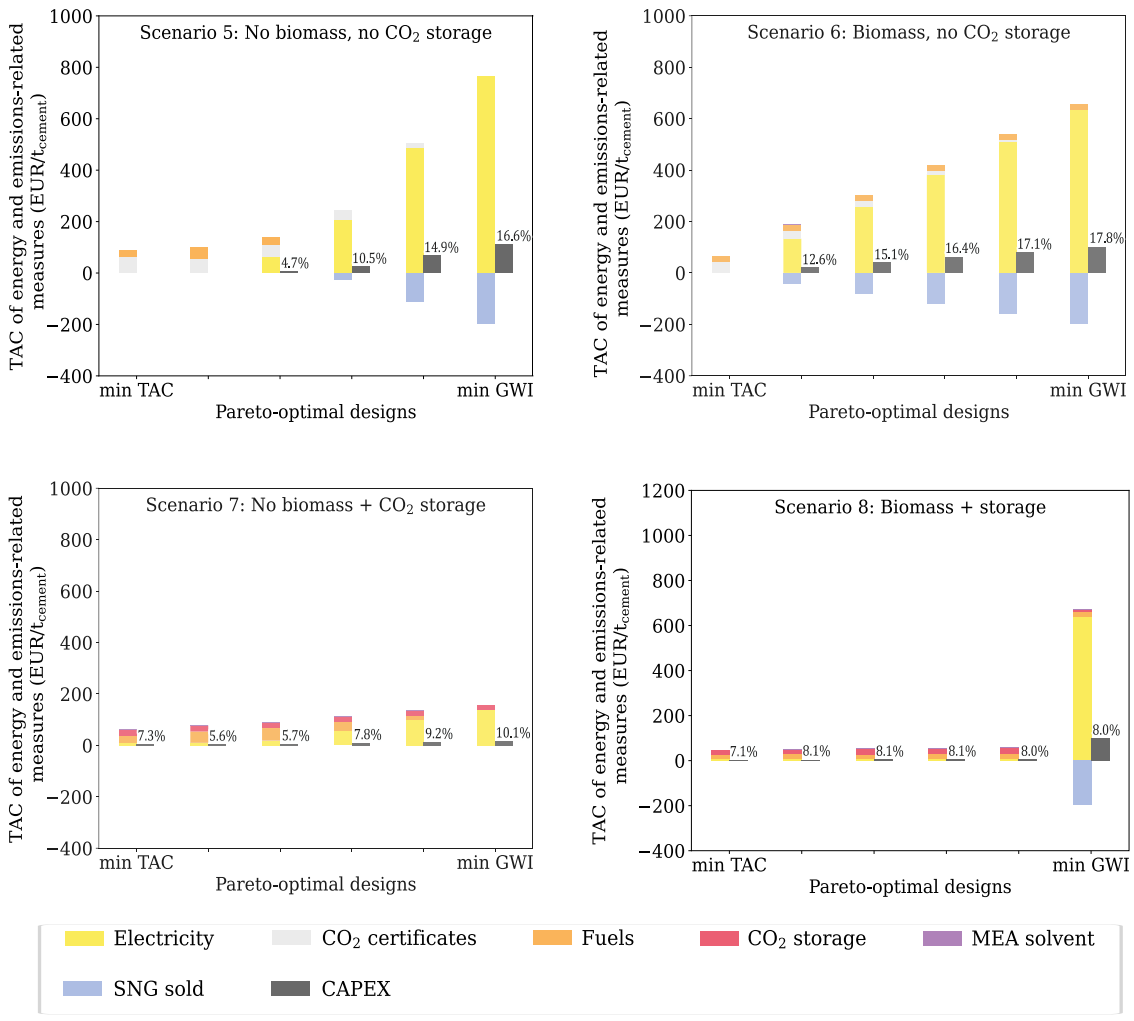

Fig. 10. TAC breakdown. The percentages displayed above the gray CAPEX bars represent the proportion of the CAPEX relative to the TAC. The stacked bars show operational costs, which include expenses for electricity, CO_2 certificates, fuels, and solvents. Negative values indicate revenues from the sale of SNG.

of biomass supply (from 0% to 100%) influence the Pareto-optimal designs.

As discussed in Section 4.2, biomass is preferred over coal, natural gas, and hydrogen from both economic and environmental perspectives. We find that, in general, variations in biomass availability primarily affect the optimal fuel mix, while the preference between CCU and CCS technologies remains unchanged. That is, CCU and CCS technologies remain the optimal options in Scenarios 6 and 8, respectively, regardless of biomass availability.

Fig. 13 shows that fuels with lower carbon intensity are selected to minimize GWI, with a transition from coal to natural gas (Scenarios 6 and 8) and subsequently from natural gas to hydrogen (Scenario 6). In Scenario 8, when biomass availability is limited to 30% and 60%, the combination of coal and biomass is preferred across most Pareto-optimal designs, with variations only in the amount of CO_2 captured. A fuel mix of natural gas and biomass is selected only in low-GWI designs, where natural gas combustion leads to lower direct and indirect emissions compared to coal. Furthermore, in low-TAC designs under partial biomass availability, (30% and 60%), the fuel mix consists of coal and biomass, highlighting biomass as a more economically option than coal.

5. Conclusion

We determine optimal combinations of options for GHG emission mitigation in retrofitting OPC production with regard to economic and environmental performance by means of superstructure optimization. To this end, we consider eight scenarios that differ with respect to the availability of biomass as a fuel, the availability of carbon storage, and the emission factor of the electricity mix.

Our results show that the optimal combination of CCUS technologies and fuel substitution in retrofitted OPC production strongly depends on the local conditions. For the current German electricity mix, the GWI can be reduced by 37.6% by replacing fossil fuels with biomass, and by 98.2% if carbon storage would be available. For a low-emission electricity mix like the one of Norway, a combination of CCU technologies and biomass as fuel reduces the GWI by 68% compared to the BAT plant, while the integration of CCS technologies with biomass enables negative GWIs, down to a value of −0.3 t $CO_{2_{eq}}$/t cement. Such low GWI values would make the cement industry carbon negative, a finding that is in line with other studies (International Energy Agency (IEA) Bioenergy, 2021; Cavalett et al., 2022). However, sufficient amounts of biomass and a supply of low-carbon electricity will be crucial for achieving such ambitious goals.

Our analysis shows that implementing CCS is generally more economically and environmentally viable than CCU technologies based on power-to-methane technologies. While the TAC for CCS range from 48 to 172 EUR/t cement, the TAC for CCU reach extreme values ranging between 166 and 680 EUR/t cement, assuming an electricity price of 128 EUR/MWh. By far, the largest share of the TAC for designs considering CCU technologies lies in the electricity costs. Only very low electricity prices (20 EUR/MWh) give rise to Pareto-optimal

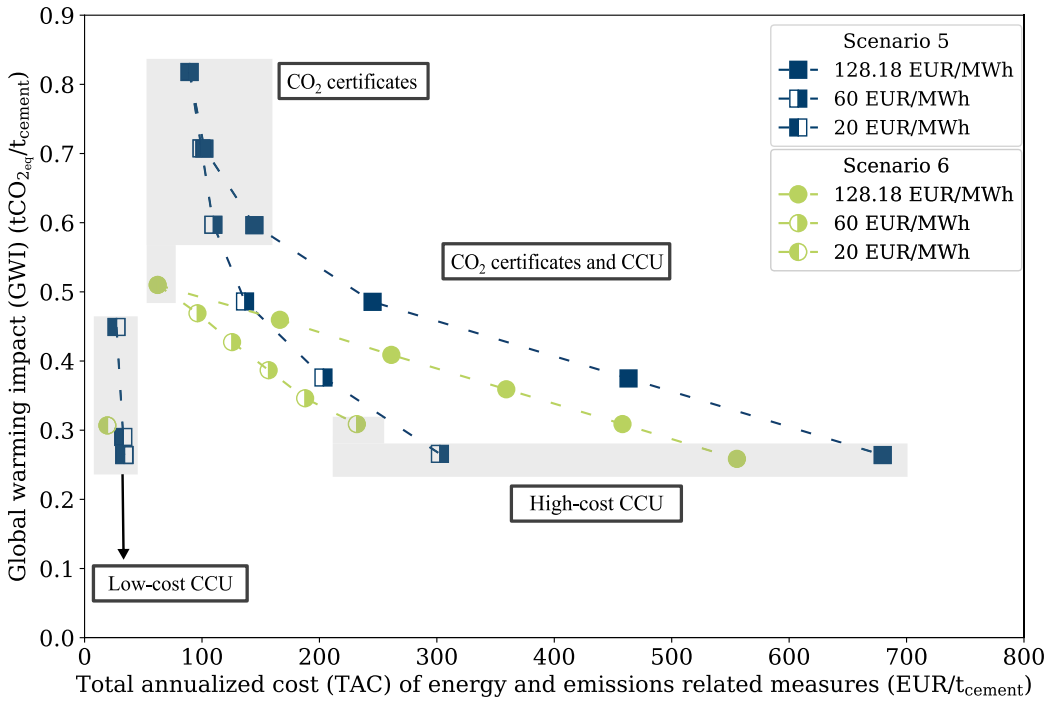

Fig. 11. Pareto fronts for Scenarios 5 and 6 that prompt installation of electricity-intense CCU technologies, assuming three different electricity prices.

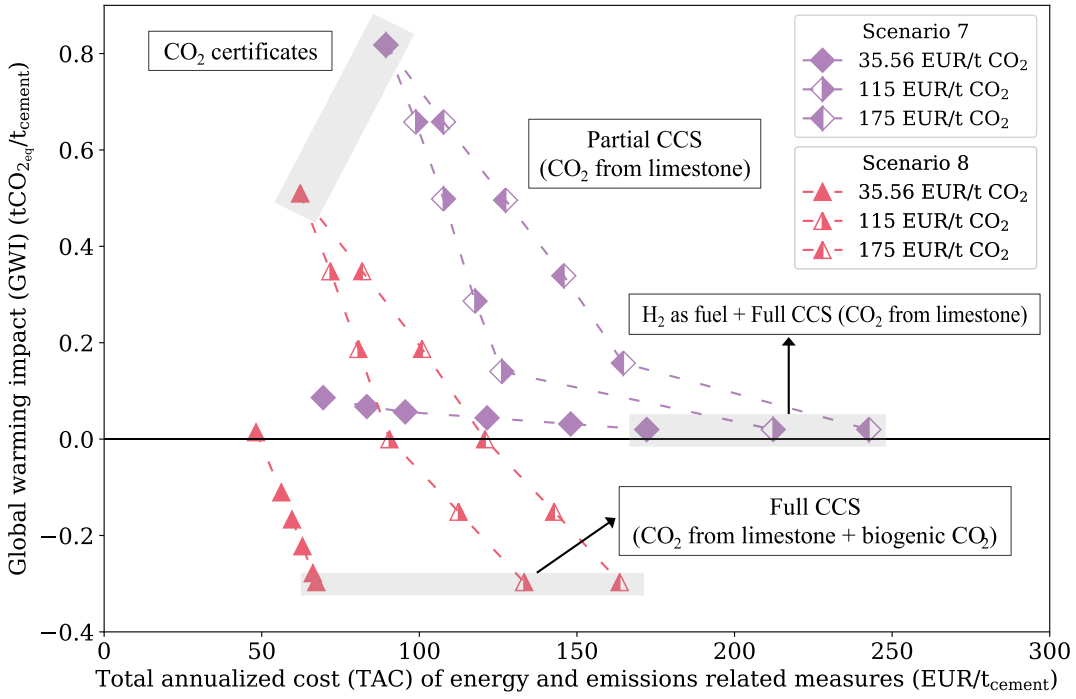

Fig. 12. Pareto fronts for Scenarios 7 and 8, assuming three different CO_2 storage costs. The Pareto fronts for Scenario 7, except for the CO_2 storage cost of 35.56 EUR/t CO_2, resemble an L-shaped curve.

designs that utilize CCU technologies instead of solely paying for CO_2 certificates.

With the economic and environmental impacts of the retrofitted OPC production process strongly depending on the plant location, the parameters of the superstructure optimization problem should be adapted to the local conditions and constraints of a particular plant under consideration. Moreover, we have restricted the superstructure to mid- and high-TRL technologies, i.e., widely studied technologies. To also include emerging (low-TRL) technologies, predictive cost correlations need to be derived. Given the low economic potential of the CCU technologies currently included in the superstructure, the addition of products other than SNG should be considered. Sick et al. (2022) project that by 2050 aggregates, precast concrete, jet fuel, and methanol are expected to be the CCU products with the highest revenue potential. It should be noted that the deployment of carbon storage is not without its challenges. In particular, CO_2 leakage from CCS

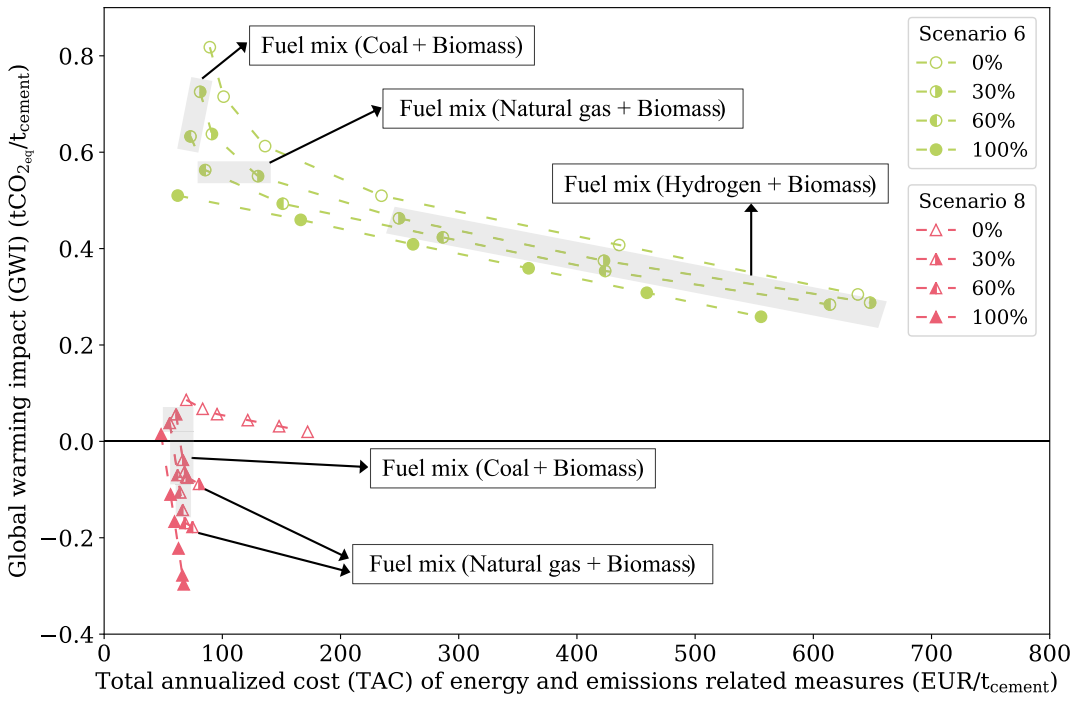

Fig. 13. Pareto fronts for Scenarios 6 and 8 considering biomass availability levels of 0%, 30%, 60% and 100%.

technologies could represent an issue and lead to additional indirect emissions (Vinca et al., 2018). To minimize the risk of CO_2 leakage and ensure the integrity of storage sites, continuous monitoring, during and after injection, is essential (Gholami et al., 2021).

Finally, our analysis shows that CCS technologies are crucial for cement plants to achieve net-zero or even negative CO_2 emissions (if biomass is available). However, emerging CCU technologies other than PtMe, notably carbon mineralization, could become economically and environmentally viable alternatives (Driver et al., 2024; Bremen et al., 2022). Besides the reduction in GHG emissions, there is a need in the concrete and cement industry for sustainable material cycles, motivating the integration of material flows and transformation units, e.g., for mineral carbonation (Zajac et al., 2022), into the superstructure approach.

CRediT authorship contribution statement

Ariana Y. Ojeda-Paredes: Writing – original draft, Visualization, Software, Methodology, Investigation, Conceptualization. **Alexander Mitsos:** Writing – review & editing, Supervision, Funding acquisition, Conceptualization. **Manuel Dahmen:** Writing – review & editing, Supervision, Methodology, Funding acquisition, Conceptualization.

Declaration of competing interest

The authors declare that they have no known competing financial interests or personal relationships that could have appeared to influence the work reported in this paper.

Acknowledgments

We would like to thank Peter Stermmermann (Karlsruhe Institute of Technology, Institute for Technical Chemistry (ITC)) for providing and recommending literature on efficient cement processing technologies. This work was funded by the Helmholtz Association of German Research Centers through program-oriented funding and the Innovation Pool projects “Energiewende und Kreislaufwirtschaft” (energy transition and circular economy) and “Industrielle Transformation 2050” (industrial transformation 2050).

Appendix A. Supplementary data

Supplementary material related to this article can be found online at https://doi.org/10.1016/j.compchemeng.2025.109200.

Data availability

No data was used for the research described in the article.

References

Abanades, J.C., Rubin, E.S., Mazzotti, M., Herzog, H.J., 2017. On the climate change mitigation potential of co2 conversion to fuels. Energy Env. Sci. 10, 2491–2499.

Abbasi, T., Abbasi, S., 2010. Biomass energy and the environmental impacts associated with its production and utilization. Renew. Sustain. Energy Rev. 14, 919–937.

Alie, C., 2004. CO_2 Capture with MEA: Integrating the Absorption Process and Steam Cycle of an Existing Coal-Fired Power Plant (Master’s thesis). https://www.collectionscanada.gc.ca/obj/s4/f2/dsk3/OWTU/TC-OWTU-450.pdf. (Accessed 10 2023).

Anderson, S., Newell, R., 2004. Prospects for carbon capture and storage technologies. Annu. Rev. Environ. Resour. 29, 109–142.

Bacatelo, M., Capucha, F., Ferrão, P., Margarido, F., 2023. Selection of a CO_2 capture technology for the cement industry: An integrated TEA and LCA methodological framework. J. CO_2 Util. 68, 102375.

Barbhuiya, S., Kanavaris, F., Das, B.B., Idrees, M., 2024. Decarbonising cement and concrete production: Strategies, challenges and pathways for sustainable development. J. Build. Eng. 86, 108861.

BASIS, 2015. European wood chips plants - country analysis. BASIS – biomass availability and sustainability information system. In: BASIS Project Is Supported By the Intelligent Energy Europe Program (IEE/12/830/S12.645698). https://www.fachverband-holzenergie.de/downloads/publikationen. (Accessed 27 March 2024).

Beguedou, E., Narra, S., Afrakoma Armoo, E., Agboka, K., Damgou, M.K., 2023. Alternative fuels substitution in cement industries for improved energy efficiency and sustainability. Energies 16 (3533).

Biegler, L.T., Grossmann, I.E., Westerberg, A.W., 1997. Systematic methods of chemical process design. In: Prentice Hall International Series in the Physical and Chemical Engineering Sciences. Prentice Hall, Upper Saddle River, NJ, 1997.

Bremen, A.M., Strunge, T., Ostovari, H., Spütz, H., Mhamdi, A., Renforth, P., van der Spek, M., Bardow, A., Mitsos, A., 2022. Direct olivine carbonation: Optimal process design for a low-emission and cost-efficient cement production. Ind. Eng. Chem. Res. 61, 13177–13190.

Bundesnetzagentur and Bundeskartellamt, 2022. Monitoringbericht 2022. Report. Bundesnetzagentur und bundeskartellamt. https://www.bundesnetzagentur.de/DE/Fachthemen/ElektrizitaetundGas/Monitoringberichte/start.html. (Accessed 03 August 2023).

Bundesnetzagentur and Bundeskartellamt, 2023. Monitoringbericht 2023. Report. Bundesnetzagentur und bundeskartellamt. https://www.bundesnetzagentur.de/DE/Fachthemen/ElektrizitaetundGas/Monitoringberichte/start.html. (Accessed 15 February 2024).

Bundesnetzagentur|SMARD.de, 2023. SMARD strommarktdaten. URL: https://www.smard.de/. (Accessed 15 February 2024).

Buttler, A., Spliethoff, H., 2018. Current status of water electrolysis for energy storage, grid balancing and sector coupling via power-to-gas and power-to-liquids: A review. Renew. Sustain. Energy Rev. 82, 2440–2454.

C.A.R.M.E.N.e.V., 2023. Marktpreise hackschnitzel. https://www.carmen-ev.de/ (Accessed 28 March 2024).

Cavalett, O., Watanabe, M.D.B., Fleiger, K., Hoenig, V., Cherubini, F., 2022. LCA and negative emission potential of retrofitted cement plants under oxyfuel conditions at high biogenic fuel shares. Sci. Rep. 12, 2045–2322.

CEMBUREAU The European Cement Association, 2020. Cementing the European green deal. Reaching climate neutrality along the cement and concrete value chain by 2050. https://cembureau.eu/library/reports/2050-carbon-neutrality-roadmap/. (Accessed 09 August 2024).

CEMEX, 2021. CEMEX successfully deploys hydrogen-based ground-breaking technology. https://www.worldcement.com/europe-cis/23022021/cemex-to-deploy-hydrogen-technology-throughout-its-cement-operations/. (Accessed 30 January 2023).

Cevik, S., Ninomiya, K., 2023. Chasing the sun and catching the wind: Energy transition and electricity prices in Europe. J. Econ. Financ. 47, 912–935.

Chauvy, R., Dubois, L., Lybaert, P., Thomas, D., De Weireld, G., 2020. Production of synthetic natural gas from industrial carbon dioxide. Appl. Energy 260, 114249.

Chen, L.Y., Adi, V.S.K., Laxmidewi, R., 2022. Shell and tube heat exchanger flexible design strategy for process operability. Case Stud. Therm. Eng. 37, 102163.

Clean Air Task Force (CATF), 2023. Mapping the cost of carbon capture and storage in europe. https://www.catf.us/2023/02/mapping-cost-carbon-capture-storage-europe/. (Accessed 16 May 2024).

Delmelle, R., Heel, A., 2020. Methanation of cement-based CO_2 emissions without prior CO_2 separation. Report. zürcher hochschule für angewandte wissenschaft. https://www.cemsuisse.ch/app/uploads/2020/04/201803_Schlussbericht_Methanation-of-cement.pdf . (Accessed 25 January 2024).

Deolalkar, S.P., 2009. Handbook for Designing Cement Plants. BS Publications, Hyderabad, India.

Ding, X., Chen, H., Li, J., Zhou, T., 2023. Comparative techno-economic analysis of CO_2 capture processes using blended amines. Carbon Capture Sci. Technol. 9, 100136.

Domingos, M.E.G.R., Flórez-Orrego, D., Teles dos Santos, M., de Oliveira Júnior, S., Maréchal, F., 2023. Multi-time integration approach for combined pulp and ammonia production and seasonal CO_2 management. Comput. Chem. Eng. 176, 108305.

Driver, J.G., Bernard, E., Patrizio, P., Fennell, P.S., Scrivener, K., Myers, R.J., 2024. Global decarbonization potential of co₂ mineralization in concrete materials. Proc. Natl. Acad. Sci. 121, e2313475121.

Driver, J.G., Hills, T., Hodgson, P., Sceats, M., Fennell, P.S., 2022. Simulation of direct separation technology for carbon capture and storage in the cement industry. Chem. Eng. J. 449, 137721.

Dutcher, B., Fan, M., Russell, A.G., 2015. Amine-based CO_2 capture technology development from the beginning of 2013-a review. ACS Appl. Mater. Interfaces 7–4, 2137–2148.

ECRA, 2009. ECRA CCS Project—Report About Phase II. Report TR-ECRA-106/2009, European Cement Research Academy GmbH, https://ecra-online.org/search/?q=technical+report+phase+II. (Accessed 10 October 2021).

EEX, 2023. Emission Spot Primary Market Auction Report 2021. Report, European Energy Exchange, https://Www.Eex.Com/En/Market-Data/Environmental-Markets/Eua-Primary-Auction-Spot-Download. (Accessed 15 February 2024).

El-Emam, R.S., Gabriel, K.S., 2021. Synergizing hydrogen and cement industries for Canada's climate plan – case study. Energy Sour. Part A: Recovery Util. Environ. Effects 43, 3151–3165.

EU Commission, 2011. Energy Roadmap 2050. Impact Assessment and Scenario Analysis. Report SEC, 1565. EU, https://Energy.Ec.Europa.Eu/System/Files/2014-10/Roadmap2050_ia_20120430_en_0.Pdf. (Accessed 04 September 2024).

Faria, D.G., Carvalho, M.M., Neto, M.R., de Paula, E.C., Cardoso, M., Vakkilainen, E.K., 2022. Integrating oxy-fuel combustion and power-to-gas in the cement industry: A process modeling and simulation study. Int. J. Greenh. Gas Control. 114, 103602.

Favier, A., De Wolf, C., Scrivener, K., Habert, G., 2018. A Sustainable Future for the European Cement and Concrete Industry: Technology Assessment for Full Decarbonisation of the Industry By 2050. Technical Report, ETH Zurich, https://www.research-collection.ethz.ch/handle/20.500.11850/301843. (Accessed 04 August 2024).

Fierro, J.J., Escudero-Atehortua, A., Nieto-Londoño, C., Giraldo, M., Jouhara, H., Wrobel, L.C., 2020. Evaluation of waste heat recovery technologies for the cement industry. Int. J. Thermofluids 7-8, 100040.

Gardarsdottir, S.O., De Lena, E., Romano, M., Roussanaly, S., Voldsund, M., Pérez-Calvo, J.F., Berstad, D., Fu, C., Anantharaman, R., Sutter, D., Gazzani, M., Mazzotti, M., Cinti, G., 2019. Comparison of technologies for CO_2 capture from cement production— part 2: cost analysis. Energies 12 (542).

GCCA, 2021. GNR 2.0 – GCCA in numbers. https://gccassociation.org/sustainability-innovation/gnr-gcca-in-numbers/. (Accessed 21 January 2024).

Ghaib, K., Ben-Fares, F.Z., 2018. Power-to-methane: A state-of-the-art review. Renew. Sustain. Energy Rev. 81, 433–446.

Gholami, R., Raza, A., Iglauer, S., 2021. Leakage risk assessment of a CO_2 storage site: A review. Earth-Sci. Rev. 223, 103849.

Global CCS Institute, 2021. Technology Readiness and Costs of CCS. Report, https://www.globalccsinstitute.com/wp-content/uploads/2021/03/Technology-Readiness-and-Costs-for-CCS-2021-1.pdf . (Accessed 08 September 2023).

Gorre, J., Ruoss, F., Karjunen, H., Schaffert, J., Tynjälä, T., 2020. Cost benefits of optimizing hydrogen storage and methanation capacities for power-to-gas plants in dynamic operation. Appl. Energy 257, 113967.

Götz, M., Lefebvre, J., Mörs, F., McDaniel Koch, F., Bajohr, S., Reimert, R., Kolb, T., 2016. Renewable power-to-gas: A technological and economic review. Renew. Energy 85, 1371–1390.

Grammelis, P., Margaritis, N., Karampinis, E., 2016. Solid Fuel Types for Energy Generation: Coal and Fossil Carbon-Derivative Solid Fuels. Woodhead Publishing, Boston, pp. 29–58, chapter 2.

Grossmann, I.E., Aguirre, P.A., Barttfeld, M., 2004. Optimal synthesis of complex distillation columns using rigorous models. In: Barbosa-Póvoa, A., Matos, H. (Eds.), European Symposium on Computer-Aided Process Engineering-14. Elsevier, pp. 53–74.

Grossmann, I.E., Guillén-Gosálbez, G., 2010. Scope for the application of mathematical programming techniques in the synthesis and planning of sustainable processes. Comput. Chem. Eng. 34, 1365–1376, Selected papers from the 7th International Conference on the Foundations of Computer-Aided Process Design (FOCAPD, 2009, Breckenridge, Colorado, USA.

Gurobi Optimization, LLC, 2020. Gurobi optimizer version 9.5.1. http://www.gurobi.com (Accessed 01 June 2021).

Hasanbeigi, A., Price, L., Lin, E., 2012. Emerging energy-efficiency and CO_2 emission-reduction technologies for cement and concrete production: A technical review. Renew. Sustain. Energy Rev. 16, 6220–6238.

HeidelbergCement, 2020. Heidelbergcement and partners drive innovative CO_2 separation. https://www.heidelbergmaterials.com/en/pr-30-03-2020. (Accessed 21 October 2021).

Hills, T., Leeson, D., Florin, N., Fennell, P., 2016. Carbon capture in the cement industry: Technologies, progress, and retrofitting. Environ. Sci. Technol. 50, 368–377.

Holladay, J., Hu, J., King, D., Wang, Y., 2009. An overview of hydrogen production technologies. Catal. Today 139, 244–260.

Hossain, M.U., Poon, C.S., Kwong Wong, A., 2019. Techno-environmental feasibility of wood waste derived fuel for cement production. J. Clean. Prod. 230, 663–671.

Icha, P., Lauf, T., 2022. Entwicklung der spezifischen Treibhausgas-Emissionen des deutschen Strommix in den Jahren 1990-2022. Report Climate Change 15/2022, Umweltbundesamt, https://www.umweltbundesamt.de/publikationen/entwicklung-der-spezifischen-treibhausgas-9. (Accessed 15 February 2024).

Ige, O.E., Von Kallon, D.V., Desai, D., 2024. Carbon emissions mitigation methods for cement industry using a systems dynamics model. Clean Technol. Environ. Policy 26, 579–597.

Intergovernmental Panel on Climate Change (IPCC), 2014. Climate change 2014: Mitigation of climate change. In: Working Group III Contribution To the Fifth Assessment Report of the Intergovernmental Panel on Climate Change. Cambridge University Press, Cambridge, United Kingdom and New York, NY, USA.

International Energy Agency-Greenhouse Gas R&D Programme (IEA-GHG), 2013. Deployment of CCS in the Cement Industry. Report 2013/19, https://ieaghg.org/docs/General_Docs/Reports/2013-19.pdf . (Accessed 10 October 2021).

International Energy Agency (IEA), 2018. Technology Roadmap - Low-Carbon Transition in the Cement Industry. Report, https://www.iea.org/reports/technology-roadmap-low-carbon-transition-in-the-cement-industry . (Accessed 10 October 2021).

International Energy Agency (IEA), 2020. Technology Perspectives Energy Special Report on Carbon Capture Utilisation and Storage (CCUS) in Clean Energy Transitions. Report, https://www.iea.org/reports/ccus-in-clean-energy-transitions/ccus-technology-innovation. (Accessed 22 August 2021).

International Energy Agency (IEA), 2022. Norway 2022. Energy Policy Review. Report, https://www.iea.org/reports/norway-2022/executive-summary. (Accessed 22 March 2023).

International Energy Agency (IEA), 2023. Bioenergy with carbon capture and storage. https://www.iea.org/energy-system/carbon-capture-utilisation-and-storage/bioenergy-with-carbon-capture-and-storage . (Accessed 20 March 2024).

International Energy Agency (IEA) Bioenergy, 2021. Deployment of Bio-CCS in the Cement Sector: An Overview of Technology Options and Policy Tools. Report, https://www.ieabioenergy.com/wp-content/uploads/2022/03/bio-CCS-in-the-cement-sector.pdf. (Accessed 20 March 2024).

Ishak, S.A., Hashim, H., 2015. Low carbon measures for cement plant - a review. J. Clean. Prod. 103, 260–274.

Jering, A., Klatt, A., Seven, J., Ehlers, K., Günther, J., Ostermeier, A., Mönch, L., 2013. Sustainable use of global land and biomass resources. Umweltbundesamt. https://www.umweltbundesamt.de/publikationen/sustainable-use-of-global-land-biomass-resources. (Accessed 12 July 2024).

Juangsa, F.B., Cezeliano, A.S., Darmanto, P.S., Aziz, M., 2022. Thermodynamic analysis of hydrogen utilization as alternative fuel in cement production. South Afr. J. Chem. Eng. 42, 23–31.

Karakaya, E., Nuur, C., Assbring, L., 2018. Potential transitions in the iron and steel industry in Sweden: towards a hydrogen-based future?. J. Clean. Prod. 195, 651–663.

Kenkel, P., Wassermann, T., Rose, C., Zondervan, E., 2021. A generic superstructure modeling and optimization framework on the example of bi-criteria power-to-methanol process design. Comput. Chem. Eng. 150, 107327.

Khurana, S., Banerjee, R., Gaitonde, U., 2002. Energy balance and cogeneration for a cement plant. Appl. Therm. Eng. 22, 485–494.

Knudsen, J.C., 2019. Carbon capture utilization and storage (CCUS). https://www.akersolutions.com/globalassets/investors/presentations/aker-solutions-carbon-capture-nov-2019.pdf . (Accessed 25 January 2024).

Knudsen, J.N., Jensen, J.N., Vilhelmsen, P.J., Biede, O., 2009. Experience with CO_2 capture from coal flue gas in pilot-scale: Testing of different amine solvents. Energy Procedia 1, 783–790.

Kokossis, A.C., Floudas, C.A., 1991. Synthesis of isothermal reactor—separator—recycle systems. Chem. Eng. Sci. 46, 1361–1383.

Kolb, S., Dillig, M., Plankenbühler, T., Karl, J., 2020. The impact of renewables on electricity prices in Germany - an update for the years 2014–2018. Renew. Sustain. Energy Rev. 134, 110307.

Koornneef, J., van Keulen, T., Faaij, A., Turkenburg, W., 2008. Life cycle assessment of a pulverized coal power plant with post-combustion capture, transport and storage of CO_2. Int. J. Greenh. Gas Control. 2, 448–467.

Kopp, M., Coleman, D., Stiller, C., Scheffer, K., Aichinger, J., Scheppat, B., 2017. Energiepark mainz: Technical and economic analysis of the worldwide largest power-to-gas plant with PEM electrolysis. Int. J. Hydrog. Energy 42, 13311–13320.

KPMG, 2021. Cost of Capital Study 2021. Report, KPMG AG, https://kpmg.com/de/en/home/insights/2021/10/cost-of-capital-study-2021.html . (Accessed 08 September 2023).

Kuptz, D., Hartmann, H., 2014. Qualität aus bayern physikalische eigenschaften von waldhackschnitzeln nach DIN EN ISO 17225. https://www.waldwissen.net/en/forestry/timber-and-markets/wood-energy/qualitaet-von-waldhackschnitzeln.(Accessed 18 April 2024).

Langiu, M., Shu, D.Y., Baader, F.J., Hering, D., Bau, U., Xhonneux, A., Müller, D., Bardow, A., Mitsos, A., Dahmen, M., 2021. COMANDO: A next-generation open-source framework for energy systems optimization. Comput. Chem. Eng. 152, 107366.

Lazou, A.A., Papatsoris, A.D., 2000. The economics of photovoltaic stand-alone residential households: A case study for various European and mediterranean locations. Sol. Energy Mater. Sol. Cells 62, 411–427.

Lee, U., Burre, J., Caspari, A., Kleinekorte, J., Schweidtmann, A.M., Mitsos, A., 2016. Techno-economic optimization of a post-combustion CO_2 capture process using superstructure and rigorous model. Ind. Eng. Chem. Res. 55, 12014–12026.

van Leeuwen, C., Zauner, A., 2018. Innovative Large-Scale Energy Storage Technologies and Power-To-Gas Concepts After Optimisation: Report on the Costs Involved with PtG Technologies and their Potentials Across the EU. D8.3. Technical Report, European Commission CORDIS, URL: https://cordis.europa.eu/project/id/691797/results. (Accessed 21 October 2021).

Luc, D.T., 2008. Pareto Optimality, in: Pareto Optimality, Game Theory and Equilibria. Springer, New York, NY, pp. 481–515, chapter 18.

Luo, Z., Song, H., Huang, Y., Jin, B., 2024. Recent advances on the uses of biomass alternative fuels in cement manufacturing process: A review. Energy Fuels 38, 7454–7479.

Ma, H., Tingelstad, P., Chen, D., 2023. Lactic acid production by catalytic conversion of glucose: An experimental and techno-economic evaluation. Catal. Today 408, 2–8.

Marmier, A., 2023. Decarbonisation Options for the Cement Industry. Publications Office of the European Union, Luxembourg, http://dx.doi.org/10.2760/174037, (Accessed 04 September 2024).

Mavrotas, G., 2009. Effective implementation of the ϵ-constraint method in multi-objective mathematical programming problems. Appl. Math. Comput. 213, 455–465.

Metz, B., Davidson, O., De Coninck, H., Loos, M., Meyer, L., 2005. Carbon Dioxide Capture and Storage: Special Report of the Intergovernmental Panel on Climate Change. Cambridge University Press.

Möller, B., Nielsen, P.S., 2007. Analysing transport costs of danish forest wood chip resources by means of continuous cost surfaces. Biomass Bioenergy 31, 291–298.

Naranjo, M., Brownlow, D.T., Garza, A., 2011. CO_2 capture and sequestration in the cement industry. Energy Procedia 4, 2716–2723.

Nhuchhen, D.R., Sit, S.P., Layzell, D.B., 2021. Alternative fuels co-fired with natural gas in the pre-calciner of a cement plant: Energy and material flows. Fuel 295, 120544.

Nussbaumer, T., 2003. Combustion and co-combustion of biomass: Fundamentals, technologies, and primary measures for emission reduction. Energy Fuels 17, 1510–1521.

Ozturk, M., Dincer, I., 2022. Utilization of waste heat from cement plant to generate hydrogen and blend it with natural gas. Int. J. Hydrog. Energy 47, 20695–20704.

Pahle, M., Sitarz, J., Osorio, S., Gorlach, B., 2022. The EU-ETS price through 2030 and beyond: A closer look at drivers, models, and assumptions. Input material and takeaways from a workshop in Brussels.Kopernikus-Projekt Ariadne. https://ariadneprojekt.de/media/2023/01/Ariadne-Documentation_ETSWorkshopBruessel_2022.pdf. (Accessed 12 September 2024).

Papoulias, S.A., Grossmann, I.E., 1983. A structural optimization approach in process synthesis—I: Utility systems. Comput. Chem. Eng. 7, 695–706.

Perilii, D., 2021. CCS: Co_2 capture & storage in cement. Global cement magazine. https://www.globalcement.com/magazine/articles/1232-ccs-co2-capture-storage-in-cement. (Accessed 10 August 2022).

Plaza, M.G., Martínez, S., Rubiera, F., 2020. CO_2 capture, use, and storage in the cement industry: State of the art and expectations. Energies 13, 5692.

Purr, K., Spindler, J., Brieschke, J., Damian, H.P., Frauenstein, J., Ginzky, H., Herrmann, B., Kahrl, A., Ruddigkeit, D., Messner, D., Alsleben, C., Berger, J., Dröge, S., He, L., Kleiner, L., Ulrich, M., Tambke, J., Schultz, K., 2023. Carbon Capture and Storage (CCS) - Contribution To the Discussion on Its Integration Into National Climate Action Strategies. German Environment Agency, https://www.umweltbundesamt.de/en/publikationen/carbon-capture-storage-diskussionsbeitrag. (Accessed 30 April 2024).

Quevedo Parra, S., Romano, M.C., 2023. Decarbonization of cement production by electrification. J. Clean. Prod. 425, 138913.

Rao, A.B., Rubin, E.S., Berkenpas, M.B., 2004. An Integrated Modeling Framework for Carbon Management Technologies. Report, Carnegie Mellon University (US, https://www.osti.gov/biblio/836715. (Accessed 10 August 2022).

Röben, F.T., Schöne, N., Bau, U., Reuter, M.A., Dahmen, M., Bardow, A., 2021. Decarbonizing copper production by power-to-hydrogen: A techno-economic analysis. J. Clean. Prod. 306, 127191.

Rodríguez, R., Abanades, J.C., 2012. CO_2 capture from cement plants using oxyfired precalcination and/or calcium looping. Environ. Sci. Technol. 46, 2460–2466.

Roussanaly, S., Fu, C., Voldsund, M., Anantharaman, R., Spinelli, M., Romano, M., 2017. Techno-economic analysis of MEA CO_2 capture from a cement kiln – impact of steam supply scenario. Energy Procedia 114, 6229–6239.

Schindler, A.K., Duke, S.R., Burch, T.E., Davis, E.W., Zee, R.H., Bransby, D.I., Hopkins, C., Thompson, R.L., Duan, J., Venkatasubramanian, V., Stephen, G., 2012. Alternative Fuel for Portland Cement Processing. Report, https://www.osti.gov/biblio/1064407. (Accessed 27 March 2024).

Schorcht, F., Kourti, I., Scalet, B.M., Roudier, S., Sancho, L.D., 2013. Best Available Techniques BAT Reference Document for the Production of Cement, Lime and Magnesium Oxide. Report, Industrial Emissions Directive 2010/75/EU European Commission, https://eippcb.jrc.ec.europa.eu/reference/production-cement-lime-and-magnesium-oxide. (Accessed 10 October 2021).

Sexton, A., Dombrowski, K., Nielsen, P., Rochelle, G., Fisher, K., Youngerman, J., Chen, E., Singh, P., Davison, J., 2014. Evaluation of reclaimer sludge disposal from post-combustion CO_2 capture. Energy Procedia 63, 926–939.

Sick, V., Stokes, G., Mason, F., Yu, Y.S., Van Berkel, A., Daliah, R., Gamez, O., Gee, C., Kaushik, M., 2022. Implementing CO_2 Capture and Utilization At Scale and Speed. Technical Report, University of Michigan, URL: http://dx.doi.org/10.7302/5826. (Accessed 28 March 2024).

Smith, I., 2003. Co-Utilisation of Coal and Other Fuels in Cement Kilns. Technical Report, IEA Clean Coal Centre, London, United Kingdom, URL: https://www.osti.gov/etdeweb/biblio/20390254. (Accessed 21 October 2023).

Smith, R., 2016. Chemical Process Design and Integration, Second ed. Wiley, Chichester, West Sussex, United Kingdom, 2016.

Smith, E., Morris, J., Kheshgi, H., Teletzke, G., Herzog, H., Paltsev, S., 2021. The cost of CO_2 transport and storage in global integrated assessment modeling. Int. J. Greenh. Gas Control. 109, 103367.

Thema, M., Bauer, F., Sterner, M., 2019. Power-to-gas: Electrolysis and methanation status review. Renew. Sustain. Energy Rev. 112, 775–787.

Toktarova, A., Rootzén, J., Odenberger, M., 2020. Technical Roadmap Cement Industry. Report, Mistra Carbon Exit, https://www.mistracarbonexit.com/news/2020/5/19/technical-roadmap-cement-industry . (Accessed 25 January 2024).

Uebbing, J., Rihko-Struckmann, L., Sager, S., Sundmacher, K., 2020. CO_2 methanation process synthesis by superstructure optimization. J. CO_2 Util. 40, 101228.

Vega Puga, E., Moumin, G., Neumann, N.C., Roeb, M., Ardone, A., Sattler, C., 2022. Holistic view on synthetic natural gas production: A technical, economic and environmental analysis. Energies 15, 1608.

Vereinigung der Bayerischen Wirtschaft (vbw), 2023. Internationaler energiepreisvergleich für die industrie. https://www.vbw-bayern.de/Redaktion/Frei-zugaengliche-Medien/Abteilungen-GS/Wirtschaftspolitik/2023/Downloads/vbw-Studie_Internationaler-Energiepreisvergleich_Oktober-2023.pdf. (Accessed 27 September 2024).

Vielma, J.P., Ahmed, S., Nemhauser, G., 2010. Mixed-integer models for nonseparable piecewise-linear optimization: Unifying framework and extensions. Oper. Res. 58, 303–315.

Vinca, A., Emmerling, J., Tavoni, M., 2018. Bearing the cost of stored carbon leakage. Front. Energy Res. 6–2018.

Voldsund, M., Anantharaman, R., Berstad, D., Cinti, G., De Lena, E., Fu, C., Gardarsdottir, S., Jamali, A., Pérez-Calvo, J., Romano, M., Roussanaly, S., Ruppert, J., Stallmann, O., Sutter, D., 2018a. CEMCAP comparative techno-economic analysis of CO_2 capture in cement plants (d4.6). https://www.sintef.no/globalassets/project/cemcap/2018-11-14-deliverables/d4.6-cemcap-comparative-techno-economic-analysis-of-co2-capture-in-cement-plants.pdf . (Accessed 10 October 2021).

Voldsund, M., Anantharaman, R., Berstad, D., Cinti, G., De Lena, E., Gatti, M., Gazzani, M., Hoppe, H., Martínez, I., Monteiro, J.G.M.S., Romano, M., Roussanaly, S., Schols, E., Spinelli, M., Størset, S., van Os, P., 2018b. CEMCAP framework for comparative techno-economic analysis of CO_2 capture from cement plants (d3.2). https://www.zenodo.org/record/1257112#.W8hidapPpaR . (Accessed 10 October 2021).

Voldsund, M., Gardarsdottir, S.O., Lena, E.D., Pérez-Calvo, J.F., Jamali, A., Berstad, D., Fu, C., Romano, M., Roussanaly, S., Anantharaman, R., Hoppe, H., Sutter, D., Mazzotti, M., Gazzani, M., Cinti, G., Jordal, K., 2019. Comparison of technologies for CO_2 capture from cement production— part 1: Technical evaluation. Energies 12 (559).

Volker Schneider, Rob Van der Meer, Jan Hammes, 2016. Wasserstoff als brennstoff in der zementherstellung. Patent EPA. https://patents.google.com/patent/EP3196177A1/de?oq=EP3196177A1en. (Accessed 30 January 2023).

Walker, N., Bazilian, M., Buckley, P., 2009. Possibilities of reducing CO_2 emissions from energy-intensive industries by the increased use of forest-derived fuels in Ireland. Biomass Bioenergy 33, 1229–1238.

Wang, D., Li, S., Liu, F., Gao, L., Sui, J., 2018. Post combustion CO_2 capture in power plant using low temperature steam upgraded by double absorption heat transformer. Appl. Energy 227, 603–612.

Wintershall Dea, 2022. Wintershall dea and equinor partner up for large-scale CCS value chain in the north sea. Web page.. https://wintershalldea.com/en/newsroom/wintershall-dea-and-equinor-partner-large-scale-ccs-value-chain-north-sea. (Accessed 21 August 2023).

Xu, G., Hu, Y., Tang, B., Yang, Y., Zhang, K., Liu, W., 2014. Integration of the steam cycle and CO_2 capture process in a decarbonization power plant. Appl. Therm. Eng. 73, 277–286.

Yang, F., Meerman, H., Zhang, Z., Jiang, J., Faaij, A., 2022. Integral techno-economic comparison and greenhouse gas balances of different production routes of aromatics from biomass with CO_2 capture. J. Clean. Prod. 372, 133727.

Yin, L., Li, X., Zhang, L., Li, J., 2021. Characteristics of carbon dioxide desorption from mea-based organic solvent absorbents. Int. J. Greenh. Gas Control. 104, 103224.

Zajac, M., Skocek, J., Haha, M.Ben., Deja, J., 2022. CO_2 mineralization methods in cement and concrete industry. Energies 15.

ZEP, 2011. The costs of CO_2 storage: post-demonstration CCS in the EU. In: European Technology Platform for Zero Emission Fossil Fuel Power Plants. https://zeroemissionsplatform.eu/document/the-costs-of-co2-storage. (Accessed 16 May 2024).

Zhang, X., Fu, K., Liang, Z., Yang, Z., Rongwong, W., Na, Y., 2014. Experimental studies of regeneration heat duty for CO_2 desorption from aqueous DETA solution in a randomly packed column. Energy Procedia 63, 1497–1503.

Zuberi, M.J.S., Hasanbeigi, A., Morrow, W., 2022. Electrification of industrial boilers in the USA: potentials, challenges, and policy implications. Energy Effic. 15, 70.